



**NAVAL  
POSTGRADUATE  
SCHOOL**

**MONTEREY, CALIFORNIA**

**THESIS**

**COORDINATED GUIDANCE STRATEGY FOR  
MULTIPLE USVs DURING MARITIME INTERDICTION  
OPERATIONS**

by

Hongze Alex See

September 2017

Thesis Advisor:

Co-Advisor:

Second Reader:

Oleg Yakimenko

Satadal Ghosh

Fotis Papoulias

**Approved for public release. Distribution is unlimited.**

THIS PAGE INTENTIONALLY LEFT BLANK

REPORT DOCUMENTATION PAGE			Form Approved OMB No. 0704-0188	
Public reporting burden for this collection of information is estimated to average 1 hour per response, including the time for reviewing instruction, searching existing data sources, gathering and maintaining the data needed, and completing and reviewing the collection of information. Send comments regarding this burden estimate or any other aspect of this collection of information, including suggestions for reducing this burden, to Washington headquarters Services, Directorate for Information Operations and Reports, 1215 Jefferson Davis Highway, Suite 1204, Arlington, VA 22202-4302, and to the Office of Management and Budget, Paperwork Reduction Project (0704-0188) Washington, DC 20503.				
1. AGENCY USE ONLY (Leave blank)	2. REPORT DATE September 2017	3. REPORT TYPE AND DATES COVERED Master's thesis		
4. TITLE AND SUBTITLE COORDINATED GUIDANCE STRATEGY FOR MULTIPLE USVs DURING MARITIME INTERDICTION OPERATIONS			5. FUNDING NUMBERS	
6. AUTHOR(S) Hongze Alex See				
7. PERFORMING ORGANIZATION NAME(S) AND ADDRESS(ES) Naval Postgraduate School Monterey, CA 93943-5000			8. PERFORMING ORGANIZATION REPORT NUMBER	
9. SPONSORING /MONITORING AGENCY NAME(S) AND ADDRESS(ES) N/A			10. SPONSORING / MONITORING AGENCY REPORT NUMBER	
11. SUPPLEMENTARY NOTES The views expressed in this thesis are those of the author and do not reflect the official policy or position of the Department of Defense or the U.S. Government. IRB number ___N/A___.				
12a. DISTRIBUTION / AVAILABILITY STATEMENT Approved for public release. Distribution is unlimited.			12b. DISTRIBUTION CODE	
13. ABSTRACT (maximum 200 words)  In the past few decades, various emerging and increasing threats in the maritime domain have posed a great challenge to the Coast Guard worldwide. Currently, the U.S. Department of Defense (DOD) seeks to tackle this problem using unmanned technologies and applications. In particular, unmanned surface vehicles (USVs) seem to be a good solution contributing to successful maritime interdiction missions. The strategy would be to surround the target to restrict its further maneuver. In this case, a coordinated control of the intercept time and terminal angle attitude become the two main characteristics of the intercept mission. This thesis addresses exactly this problem. It uses a systems engineering approach to analyze the problem and comes up with the best solution, which happens to be a coordinated trajectory-shaping guidance strategy involving multiple USV pursuers. The corresponding algorithms were developed and tested for different engagement geometries through a series of computer simulations. Further verification was carried out using a three-dimensional dynamic robot simulator to study the different effects while implementing the developed algorithms on an onboard autopilot. Overall, this thesis proves that using USVs with the appropriate intercept guidance for maritime interdiction missions is a viable alternative/complement to the current operations involving only manned vessels.				
14. SUBJECT TERMS maritime interdiction, unmanned surface vehicle, coordinated guidance strategy			15. NUMBER OF PAGES 93	
			16. PRICE CODE	
17. SECURITY CLASSIFICATION OF REPORT Unclassified	18. SECURITY CLASSIFICATION OF THIS PAGE Unclassified	19. SECURITY CLASSIFICATION OF ABSTRACT Unclassified	20. LIMITATION OF ABSTRACT UU	

THIS PAGE INTENTIONALLY LEFT BLANK

**Approved for public release. Distribution is unlimited.**

**COORDINATED GUIDANCE STRATEGY FOR MULTIPLE USVs DURING  
MARITIME INTERDICTION OPERATIONS**

Hongze Alex See  
Civilian, Singapore Technologies Marine Limited  
B.Eng., Nanyang Technological University, 2008

Submitted in partial fulfillment of the  
requirements for the degree of

**MASTER OF SCIENCE IN SYSTEMS ENGINEERING**

from the

**NAVAL POSTGRADUATE SCHOOL  
September 2017**

Approved by: Oleg Yakimenko  
Thesis Advisor

Satadal Ghosh  
Co-Advisor

Fotis Papoulias  
Second Reader

Ronald Giachetti  
Chair, Department of Systems Engineering

THIS PAGE INTENTIONALLY LEFT BLANK

## **ABSTRACT**

In the past few decades, various emerging and increasing threats in the maritime domain have posed a great challenge to the Coast Guard worldwide. Currently, the U.S. Department of Defense (DOD) seeks to tackle this problem using unmanned technologies and applications. In particular, unmanned surface vehicles (USVs) seem to be a good solution contributing to successful maritime interdiction missions. The strategy would be to surround the target to restrict its further maneuver. In this case, a coordinated control of the intercept time and terminal angle attitude become the two main characteristics of the intercept mission. This thesis addresses exactly this problem. It uses a systems engineering approach to analyze the problem and comes up with the best solution, which happens to be a coordinated trajectory-shaping guidance strategy involving multiple USV pursuers. The corresponding algorithms were developed and tested for different engagement geometries through a series of computer simulations. Further verification was carried out using a three-dimensional dynamic robot simulator to study the different effects while implementing the developed algorithms on an onboard autopilot. Overall, this thesis proves that using USVs with the appropriate intercept guidance for maritime interdiction missions is a viable alternative/complement to the current operations involving only manned vessels.

THIS PAGE INTENTIONALLY LEFT BLANK

# TABLE OF CONTENTS

<b>I.</b>	<b>INTRODUCTION.....</b>	<b>1</b>
<b>A.</b>	<b>MOTIVATION .....</b>	<b>2</b>
<b>B.</b>	<b>PROBLEM FORMULATION .....</b>	<b>7</b>
<b>C.</b>	<b>THESIS ORGANIZATION.....</b>	<b>8</b>
<b>II.</b>	<b>SYSTEMS ENGINEERING APPROACH .....</b>	<b>9</b>
<b>III.</b>	<b>COORDINATED TRAJECTORY-SHAPING GUIDANCE STRATEGY.....</b>	<b>13</b>
<b>A.</b>	<b>LITERATURE REVIEW .....</b>	<b>13</b>
<b>B.</b>	<b>MULTI-PURSUER INTERDICTION PROBLEM FORMULATION.....</b>	<b>14</b>
<b>1.</b>	<b>Basic Engagement Configuration.....</b>	<b>14</b>
<b>2.</b>	<b>Background of PN-based Approach Angle Control .....</b>	<b>16</b>
<b>3.</b>	<b>Background of PN-based Final Time Control.....</b>	<b>19</b>
<b>C.</b>	<b>STRATEGIES FOR INTERDICTION MISSION .....</b>	<b>19</b>
<b>1.</b>	<b>PIP Estimation for Each Pursuer.....</b>	<b>19</b>
<b>2.</b>	<b>Trajectory-Shaping Strategy for Multiple Pursuers .....</b>	<b>21</b>
<b>3.</b>	<b>Simulation Results .....</b>	<b>23</b>
<b>4.</b>	<b>Discussion of Simulation Results .....</b>	<b>33</b>
<b>IV.</b>	<b>CODE IMPLEMENTATION IN HIGH-FIDELITY SIMULATION ENVIRONMENT.....</b>	<b>35</b>
<b>A.</b>	<b>SIMULATION SOFTWARE .....</b>	<b>35</b>
<b>B.</b>	<b>MODEL INTERFACES.....</b>	<b>37</b>
<b>C.</b>	<b>TEST AND EVALUATION.....</b>	<b>39</b>
<b>D.</b>	<b>SIMULATION RESULTS.....</b>	<b>46</b>
<b>E.</b>	<b>DISCUSSION OF SIMULATION RESULTS .....</b>	<b>63</b>
<b>V.</b>	<b>CONCLUSION AND FUTURE WORK .....</b>	<b>65</b>
	<b>LIST OF REFERENCES.....</b>	<b>67</b>
	<b>INITIAL DISTRIBUTION LIST .....</b>	<b>71</b>

THIS PAGE INTENTIONALLY LEFT BLANK

## LIST OF FIGURES

Figure 1.	Jurisdictional Classifications. Source: U.S. Coast Guard (2012). .....	3
Figure 2.	Security-in-Depth. Source: U.S. Coast Guard (2012).....	3
Figure 3.	RHIB USV Equipped with CARACaS. Source: Office of Naval Research (2014). .....	5
Figure 4.	Swarming Autonomous USVs. Source: Naval Drones (2016).....	5
Figure 5.	CARACaS Control System Screenshot. Source: Naval Drones (2016).....	6
Figure 6.	An Example of the Swarming Concept. Source: Drone Trend (2014). .....	6
Figure 7.	Mission Scenario Including the Escort of a High Value Unit (HVV) by Autonomous Surface Vehicles (ASVs), and the Interception of High Speed Maneuverable Surface Targets (HSMSTs). Source: NASA Jet Propulsion Laboratory (2014). .....	7
Figure 8.	DOD SE Process of 2014. Source: Defense Acquisition University (2017).....	9
Figure 9.	The Problem Statement.....	10
Figure 10.	Operational Need Statement. ....	10
Figure 11.	Functional Decomposition of Swarm USVs System. ....	11
Figure 12.	Relationships of MOEs, MOPs, and TPMs. Source: Hernandez (2016a).....	11
Figure 13.	Planar Engagement Geometry. ....	16
Figure 14.	Examples of Pursuer Trajectory for PPN and 2pPPN. Source: Ghosh et al. (2017). ....	18
Figure 15.	Trajectories of Two Pursuers with the Same Speed to a Stationary Target (Case 1).....	25
Figure 16.	Trajectories of Two Pursuers with Different Speeds to a Stationary Target (Case 2).....	26
Figure 17.	Intercept Characteristics for Two Pursuers for Case 1. ....	27

Figure 18.	Intercept Characteristics for Two Pursuers for Case 2. ....	28
Figure 19.	Trajectories of Two Pursuers to a Non-maneuvering Target (Cases 3–5). ....	29
Figure 20.	Intercept Characteristics for Two Pursuers for Case 3. ....	30
Figure 21.	Intercept Characteristics for Two Pursuers for Case 4. ....	31
Figure 22.	Intercept Characteristics for Two Pursuers for Case 5. ....	32
Figure 23.	Clearpath Robotics Kingfisher USV. Source: Unmanned Systems Technology (2014). ....	36
Figure 24.	Gazebo Client (Simulation of Kingfisher USV in Different Worlds). Source: NPS Wiki (2017). ....	37
Figure 25.	Concept of Data Exchange in ROS. Source: MathWorks (2015). ....	38
Figure 26.	Data Exchange between ROS Nodes during the Simulation. ....	39
Figure 27.	Trajectories of the USV through Various Waypoints, in (a) Short Guidance Command Interval and (b) Long Control Command Interval. ....	42
Figure 28.	Simulink Model of Waypoint Controller. ....	43
Figure 29.	Details of Kingfisher USV Block. ....	43
Figure 30.	Details of Heading Controller Block. ....	45
Figure 31.	Trajectories of Pursuer 1 with Different Threshold Distances for Different Guidance Command Intervals (Cases 1–5). ....	47
Figure 32.	Trajectories of Pursuer 1 with Similar Threshold Distances for Different Guidance Command Intervals (Cases 6–10). ....	50
Figure 33.	Illustration on the Effects of Threshold Distance on the Final Heading and Range from Target. ....	53
Figure 34.	Velocity Profiles of Both Pursuers for Different Guidance Command Intervals. ....	55
Figure 35.	Heading Profiles of Both Pursuers for Different Guidance Command Intervals. ....	57
Figure 36.	Yaw Rate Profiles of Both Pursuers for Different Guidance Command Intervals. ....	60

## LIST OF TABLES

Table 1.	Summary of MOE, MOPs, and TPMs.....	12
Table 2.	Computation Time vs. Mission Time. ....	33
Table 3.	Guidance Command Intervals Tested.....	41
Table 4.	Overview on the Percentage or Error for Final Heading and Range with Different Threshold Distances.....	54

THIS PAGE INTENTIONALLY LEFT BLANK

## LIST OF ACRONYMS AND ABBREVIATIONS

2pPPN	two-stage pure proportional navigation
3D	three-dimensional
AOA	analysis of alternatives
CARACaS	control architecture for robotic agent command and sensing
DOD	Department of Defense
DT&E	development test & evaluation
ENU	east north up
EO	electro-optical
GPS	global positioning system
GUI	graphic user interface
ICS	incident command system
IMU	inertial measurement unit
IP	intercept point
LoS	line-of-sight
MOE	measure of effectiveness
MOP	measure of performance
MOTR	maritime operational threat response
MTS	marine transportation system
NED	north east down
NPS	Naval Postgraduate School
NRF	national response framework
PID	proportional integral derivative
PIP	predicted intercept point
PPN	pure proportional navigation
ONR	Office of Naval Research
RHIB	rigid hull inflatable boat
ROS	robot operating system
SE	systems engineering
SEP	systems engineer process
STAR	smart tissue autonomous robot

TPMs	technical performance measures
USCG	United States Coast Guard
USV	unmanned surface vehicle

## EXECUTIVE SUMMARY

Unmanned systems and autonomous systems have gradually become part of our daily lives. These technologies aim to reduce the workload of humans and increase efficiencies, eliminate human/judgment errors and eliminate risks to humans in dangerous situations. They are changing the way the world works, and serve as a capability multiplier.

“With emerging threats such as piracy, natural resources dispute, drug trafficking, and weapons proliferation, a rapid response capability is needed in all maritime regions” (Office of the Under Secretary of Defense for Acquisition, Technology and Logistics 2011). It is no surprise that DOD turns to unmanned systems to tackle the ever-growing threats. The U.S. Coast Guard faces challenges to defend and preserve the nation, given the vast maritime territory and increasing real-life threats and incidents with limited manpower and assets. This calls for some degree of autonomy. This could be mechanized by deploying some of the armed unmanned surface vehicles (USVs) to engage and interdict targets independently or cooperatively with other systems. In order to achieve a successfully maritime interdiction mission, a swarming concept is proposed in which a group of armed USV pursuers is required to achieve a desired coordinated formation relative to the target position and heading simultaneously, which assures successful containing and/or intercepting the target.

The problem addressed in this thesis has the following formulation—can swarming USVs substitute/complement/improve efficiency of detection, interdiction and engagement of the target, yet eliminate the risks to crews and boats during the interdiction operations?

Addressing this problem involves answering the following research questions:

- 1) What is the engineering approach adopted to design a solution (i.e., swarming USVs system) to counter the problem formulated?
- 2) What is the guidance strategy considered for the USVs to perform the interdiction successfully?

### 3) What are the possible factors affecting the control of the USVs?

The thesis deals with the first research question by addressing the problem from the standpoint of systems engineering (SE). The problem was reformulated in a broader systems engineering sense, followed by the identification of the operational need. Functional decomposition was performed to identify the boundary of the scope of this thesis. The evaluation measures that results from the functional decomposition and requirement analysis were key considerations during the design stage.

The thesis continues to address the second research question and explores the problem formulated from the standpoint of the optimal control theory. It presents a novel real-time-implementable guidance strategy for a group of pursuers based on PN guidance philosophy to approach simultaneously the locations sufficiently close to a moving target while maintaining a desired terminal heading. Specifically, a simple adaptive variation of the navigation gain for one of pursuers in the group is shown to be effective for a successful interdiction mission in general. The problem of having a moving target, as opposed to a stationary target, considered in Ghosh et al. (2017) *Unmanned Aerial Vehicle Guidance for an All-Aspect Approach to a Stationary Point*, is dealt with by estimating the predicted intercept point (PIP). As seen even using interpretative execution instructions (not compiled code), the executing time requires less than 3% of the duration of a maneuver. As known, compiled code runs about 100 times faster (i.e., it will take less than 0.1s to produce a solution) (Yakimenko 2000). This implies that the algorithm can be run in real-time implementation.

Finally, the thesis discusses the third research question by studying the effects of different guidance command intervals on the trajectories of the USVs through a series of simulation runs. There is no definite conclusion or recommendations to the “best” guidance command interval or threshold distance for the USVs, or any other unmanned system and robots. The expected trajectory of the unmanned platform, the platform characteristics and the type of controller used for the system, shall be the main consideration points when determining the optimal guidance command interval or threshold distance.

Overall, this thesis proves that using USVs with the appropriate intercept guidance for the maritime interdiction missions is a viable alternative/complement to the current operations involving only manned vessels.

## References

- Ghosh, Satadal, Oleg A. Yakimenko, D. T. Davis, and T. H. Chung. 2017. “Unmanned Aerial Vehicle Guidance for an All-Aspect Approach to a Stationary Point.” Accepted in *AIAA Journal of Guidance, Control, and Dynamics*.
- Office of the Under Secretary of Defense for Acquisition, Technology and Logistics. 2011. “Unmanned Systems Integrated Roadmap: FY 2011–2036.” <http://www.acq.osd.mil/sts/docs/Unmanned%20Systems%20Integrated%20Roadmap%20FY2011-2036.pdf>.
- Yakimenko, Oleg. 2000. “Direct Method for Rapid Prototyping of Near-Optimal Aircraft Trajectories.” *Journal of Guidance, Control, and Dynamics* 23(5): 865–875.

THIS PAGE INTENTIONALLY LEFT BLANK

## ACKNOWLEDGMENTS

I would like to express my most sincere gratitude to Professor Oleg Yakimenko for his guidance, patience, and support for this thesis work. In particular, the MATLAB module taught by Professor Yakimenko equipped me with the necessary skill to complete the simulation portion of this thesis. His expertise in systems engineering and autonomous systems provided me with the main framework that guided me to the successful completion of this thesis.

I would like to thank Dr. Satadal Ghosh for his coaching, unfailing support, and valuable advice throughout the whole course of this thesis work. Without the existence of his previous research work, which serves as the platform to build on, this thesis would not have been possible.

I would like to thank Associate Professor Brian Bingham for his valuable teaching in Cooperative Control of Multiple Marine Autonomous Vehicles, which provided me with the necessary knowledge about Robot Operating System (ROS) and Gazebo to perform part of the thesis works herein.

I would like to thank Professor Fotis Papoulias for providing valuable comments on this thesis amid his busy schedule.

I would like to thank my superiors, Mr. Tan Ching Eng, Senior Vice President (Engineering Design Center), and Mr. Wong Chee Seng Steve, Director (Weapons and Electronics), for their recommendations and opportunities to attend the 18-month dual master's degree program jointly organized by Temasek Defence Systems Institute of National University of Singapore and Naval Postgraduate School.

I would also like to thank the Singapore community in Monterey. Friendships were bonded and great memories been created. Their presence lessened the homesickness and this one year in Monterey would not have been so great without their company.

I would like to thank my mother, Ong Poh Gek, as well as my siblings, See Hong Sin Eric, See Siao Jun Iris, and See Siao Wei Ellis, for their unwavering care and support over the years.

In addition, I would like to thank my lovely wife, Shuian Hu, for her unwavering care and support over the years. Her encouragement has been the main source of motivation as I strived toward my goals.

## I. INTRODUCTION

Unmanned systems and autonomous systems have gradually become part of our daily lives. Use of unmanned and autonomous technologies has spread into the transportation, construction, healthcare, space, and military sectors, and beyond. Examples of such technologies include 1) Waymo, a self-driving car (previously known as Google X) (Waymo 2017); 2) 3D printed houses; 3) STAR, a robot that is capable of performing suturing, fluorescent and 3D imaging, force and submillimeter positioning, and force sensing (Leonard et al. 2014); 4) Satellite systems; and 5) Phalanx, a rapid-fire, radar-guided gun system that fires automatically at incoming air and surface threats (Raytheon 2008). These technologies aim to reduce the workload of humans and increase efficiencies, eliminate human/judgment errors and eliminate risks to humans in dangerous situations. They are changing the way the world works, and serve as a capability multiplier.

According to the Office of the Under Secretary of Defense for Acquisition, Technology and Logistics 2011 *Unmanned Systems Integrated Roadmap: FY 2011–2036* document,

The Department of Defense's vision for unmanned systems is the seamless integration of diverse unmanned capabilities that provide flexible options for operators while exploiting the inherent advantages of unmanned technologies, including persistence, size, speed, maneuverability, and reduced risk to human life. Over 90% of the information, people, goods, and services that sustain and create opportunities for regional economic prosperity flow across the maritime domain. With emerging threats such as piracy, natural resources dispute, drug trafficking, and weapons proliferation, a rapid response capability is needed in all maritime regions. DOD continues to expand the range of missions supported by unmanned systems in the maritime domain. Today's iteration of unmanned systems involves a high degree of human interaction. DOD must continue to pursue technologies and policies that introduce a higher degree of autonomy to reduce the manpower burden and reliance on full-time high-speed communications link while also reducing decision loop cycle time. The introduction of increased unmanned system autonomy must be mindful of affordability, operational utilities, technological developments, policy, public opinion, and their associated constraints. (Office of the

## A. MOTIVATION

The vision of U.S. DOD is aligned with the evolvement of the unmanned and autonomous world. With the ever-growing threats of piracy, attacks, and weapons proliferation from the adversaries in contested maritime domain, there is an increasing need to interdict a suspect/intruder successfully to ensure safety and protection of such unmanned systems.

The U.S. Coast Guard 2012 *Operations* publication 3-0 states that

The United States claims sovereignty over 3.4 million nautical square miles of maritime territory, which comprises the Marine Transportation System (MTS). The Coast Guard has defined three geographic operational areas, namely 1) Offshore, 2) Coastal and 3) Inland. The Coast Guard operational areas overlap with recognized U.S. and international geographic regimes. These regimes of ocean and airspace directly affect maritime operations by determining the degree of jurisdiction a coastal state may exercise within the regime. National waters include internal waters and territorial seas of a coastal state. International waters include waters seaward of the territorial seas of any state. (U.S. Coast Guard 2012)

Jurisdictional classifications are further described in the publication and shown in Figure 1. The U.S. Coast Guard 2012 *Operations* publication 3-0 also states that

Security-in-depth demands that Coast Guard operations be synchronized with other U.S. and international operations to respond to maritime threats with unity of effort. The Coast Guard relies on the National Response Framework (NRF), Incident Command System (ICS), and Maritime Operational Threat Response (MOTR) Plan and Protocols to synchronize U.S. response to maritime threats and incidents, including coordination with foreign governments. (U.S. Coast Guard 2012)

Figure 2 depicts how the Coast Guard forces are allocated to conduct operations across the defined Coast Guard operational areas to provide security-in-depth (U.S. Coast Guard 2012).

In four separate events in a span of only a few days since 20 January 2017, the U.S. Customs and Boarder Protection (CBP), U.S. Coast Guard and the Puerto Rico

Police Department (PRPD) working under the Caribbean Border Interagency Group (CBIG), intercepted 126 undocumented migrants from the Dominican Republic, Cuba and Haiti (U.S. Customs and Border Protection 2017).

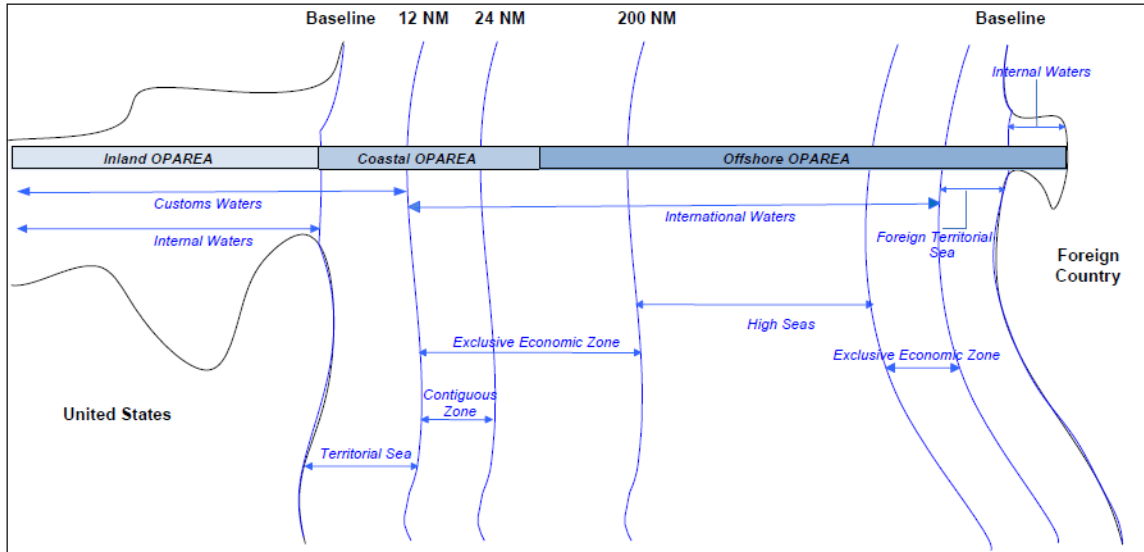


Figure 1. Jurisdictional Classifications. Source: U.S. Coast Guard (2012).

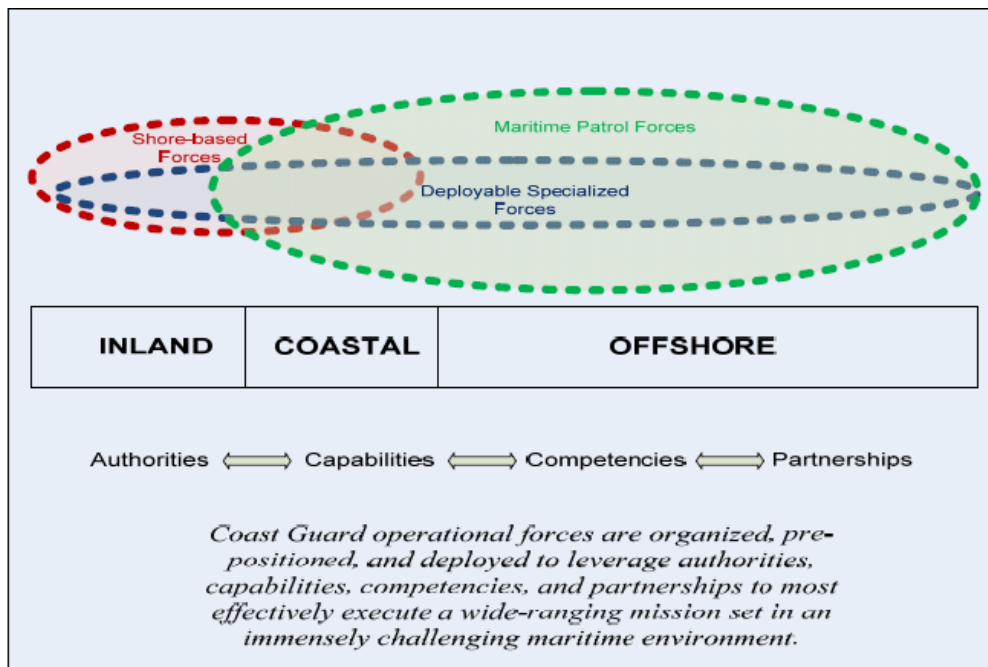


Figure 2. Security-in-Depth. Source: U.S. Coast Guard (2012).

The U.S. Coast Guard faces challenges to defend and preserve the nation, given the vast maritime territory and increasing real-life threats and incidents with limited manpower and assets. This calls for some degree of autonomy. This could be mechanized by deploying some of the armed unmanned surface vehicles (USVs) to engage and interdict targets independently or cooperatively with other systems. In order to achieve a successfully maritime interdiction mission, a swarming concept is proposed in which a group of armed USV pursuers is required to achieve a desired coordinated formation relative to the target position and heading simultaneously, which assures successful containing and/or intercepting the target.

In August 2014, the Office of Naval Research (ONR) conducted a USV swarm demonstration on the James River in Virginia with resounding success. The USVs are Rigid Hull Inflatable Boats (RHIBs) equipped with Robotic Agent Command and Sensing (CARACaS), “a platform-agnostic system under development by the ONR that can be installed in a variety of small craft transforming them into autonomous USVs” (Naval Drones 2016). As noted on their website,

As many as 13 various patrol craft were equipped with the CARACaS system to demonstrate a “swarm” escort of high value shipping in the James River. The USVs were able to autonomously take station on the escorted vessel with no external inputs using a fused-radar picture. When ordered, the swarm would break off escort to surround a contact of interest. (Naval Drones 2016)

Presented in Figures 3–7 are an example of the USV, a swarm of USVs in action, the CARACaS Control System, examples of the swarming concept, and USV use in different scenarios, respectively.

USVs are highly desired for such as the aforementioned missions because they not only directly address the dangers and concerns faced by crews in a manned interceptor boats, but also address the issues of limited resources in terms of manpower/crews and interceptor boats.



Figure 3. RHIB USV Equipped with CARACaS.  
Source: Office of Naval Research (2014).



Figure 4. Swarming Autonomous USVs. Source: Naval Drones (2016).



Figure 5. CARACaS Control System Screenshot. Source: Naval Drones (2016).



Figure 6. An Example of the Swarming Concept. Source: Drone Trend (2014).

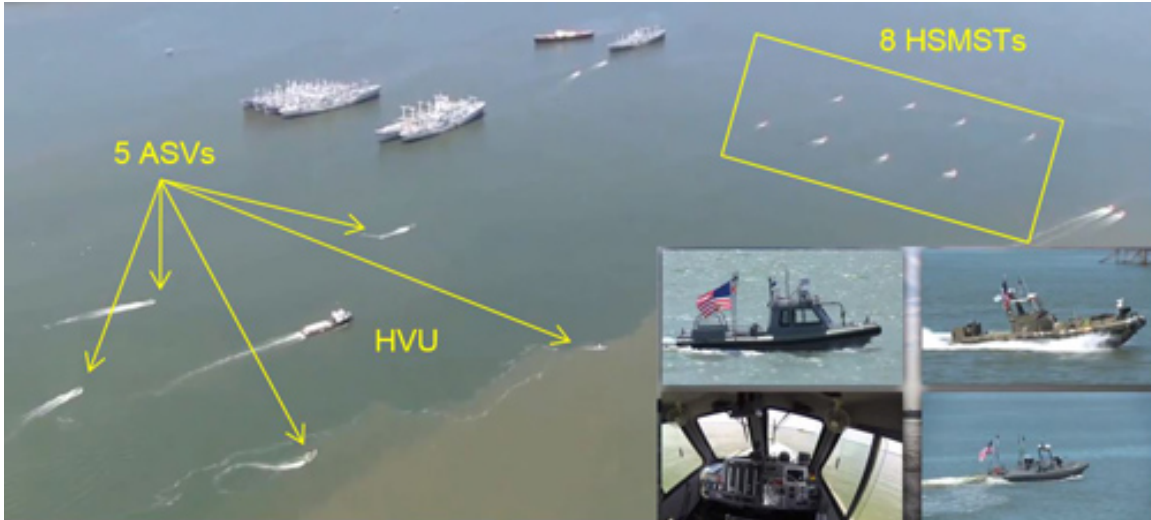


Figure 7. Mission Scenario Including the Escort of a High Value Unit (HVU) by Autonomous Surface Vehicles (ASVs), and the Interception of High Speed Maneuverable Surface Targets (HSMSTs).  
Source: NASA Jet Propulsion Laboratory (2014).

## B. PROBLEM FORMULATION

As discussed and stated in the previous sections from U.S. Coast Guard 2012 *Operations* publication 3-0,

The Coast Guard employs security-in-depth to conduct operations. Personnel and assets are deployed and stationed in layers in the offshore, coastal, and inland operational areas to prevent and respond to threats well before they reach U.S. waters and the MTS. Coast Guard forces reduce the risk of security incidents by identifying and addressing vulnerabilities to threats, then detecting, interdicting and defeating threats before they approach U.S. shores. (U.S. Coast Guard 2012, 28)

The problem addressed in this thesis has the following formulation: can swarming USVs substitute/complement/improve efficiency of detection, interdiction and engagement of the target, yet eliminate the risks to crews and boats during the interdiction operations?

Addressing this problem involves answering the following research questions:

- 1) What is the engineering approach adopted to design a solution (i.e., swarming USVs system) to counter the problem formulated?

2) What is the guidance strategy considered for the USVs to perform the interdiction successfully?

3) What are the possible factors affecting the control of the USVs?

### **C. THESIS ORGANIZATION**

To address the problem formulated in Section I.B, this thesis is organized as follows.

It continues with Chapter II dealing with the first research question. It addresses the problem from the standpoint of systems engineering (SE). An SE process model is introduced to provide the framework on the approach to the problem and guide the development of the solution.

Chapter III addresses the second research question and explores the problem formulated in Section I.B from the standpoint of the optimal control theory. This chapter details the background and theorem behind the development of the coordinated trajectory-shaping guidance algorithm, followed by the presentation of the algorithm to achieve the final time and terminal angle simultaneously. The chapter continues with the results of simulation in different scenarios and offers some discussion on the analysis of the results.

Chapter IV discusses the third research question by studying the effects of different guidance command intervals on the trajectories of the USVs through a series of simulation runs and offers some discussions on the simulation results.

Chapter V summarizes the thesis work and concludes with recommendations for further studies.

## II. SYSTEMS ENGINEERING APPROACH

This chapter introduces the systems engineering (SE) approach that is best suited to tackle the problem identified in Section I.B for the swarming USVs system. The DOD Systems Engineering Process (SEP) Model of 2014 (Defense Acquisition University 2017), depicted in Figure 8, shall provide the SE framework to guide the development of the solution.

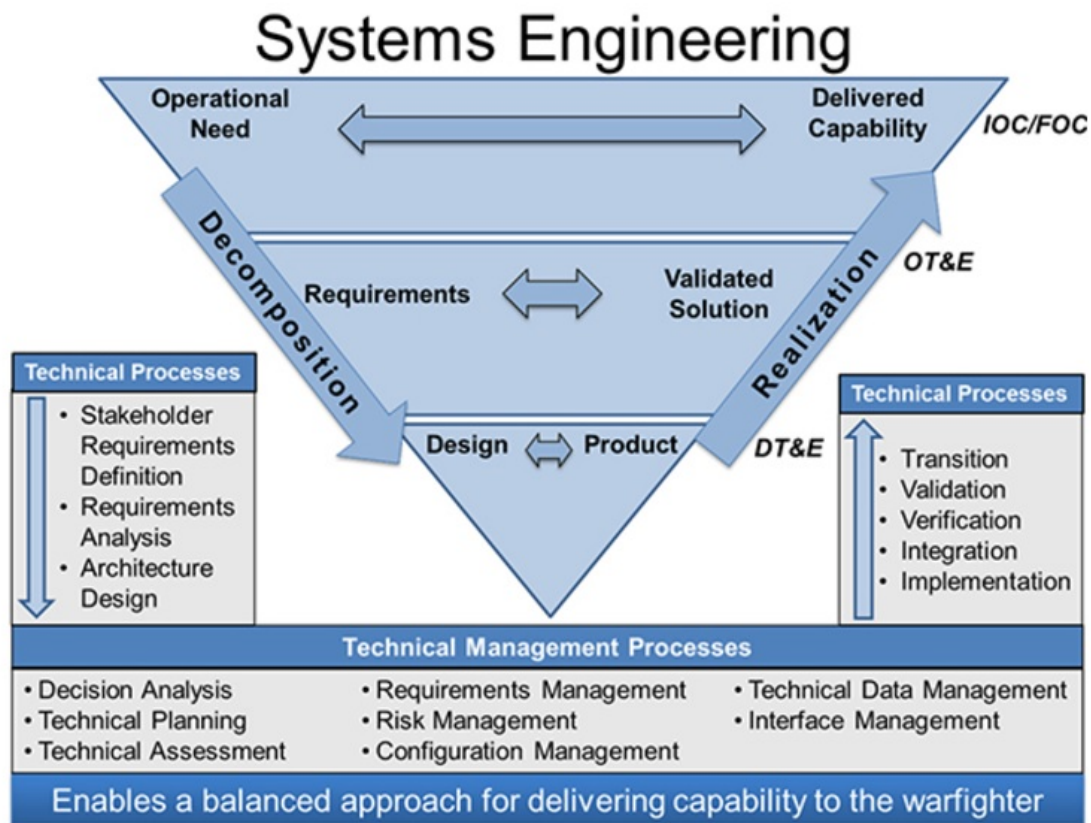


Figure 8. DOD SE Process of 2014. Source: Defense Acquisition University (2017).

Following the problem formulated in Section I.B, the problem statement identified in a broader systems engineering sense is shown in Figure 9.

*High-Speed Interdiction Operations pose a safety hazard to the crews. The crews are subjected to high risk of being thrown overboard due to heavy pounding of the interceptor boats during the interdiction operation or even at risk of capsizing. There are also limited/reasonable resources in terms of manpower and interceptor boats to interdict a suspicious target. Coordination and clear communication between interceptor boat crews to form a certain formation around the target to restrict its further maneuver is also a great challenge due to the pursuit environment.*

Figure 9. The Problem Statement.

The first step of the SEP is to establish the operational need. The operational need statement can be derived from the problem statement after needs analysis/assessment from the stated problem and is defined in Figure 10.

*The operation need is an autonomous swarm USVs system that is capable of replacing manned boats to perform interdiction operations with high success rate and eliminate any risk to the crews associated with such operations.*

Figure 10. Operational Need Statement.

A functional analysis is conducted to identify the functions of the system (i.e., what the system must do to accomplish its mission), which are essentially the system requirements (Step 2 of SEP). These system requirements are then translated into design criteria (Step 3 of SEP). The functional decomposition of the system is depicted in Figure 11. The product/sub-system, a software package that is designed and developed according to the design criteria from the functions highlighted in yellow is addressed in Chapter III and IV of this thesis. The rest of the functions, which are directly related to the design and characteristics of the USV platform, are out of the scope of this thesis.

Each function identified is associated with an evaluation measure. Evaluation measures serve as criteria to determine whether the function has been satisfactorily

implemented in the system and whether the system has accomplished mission objectives and achieved desired results (AcqNotes 2016). There are three types of evaluation measures, namely, measure of effectiveness (MOE), measure of performance (MOP), and technical performance measure (TPM). The relationship among MOEs, MOPs and TPMs is depicted in Figure 12.

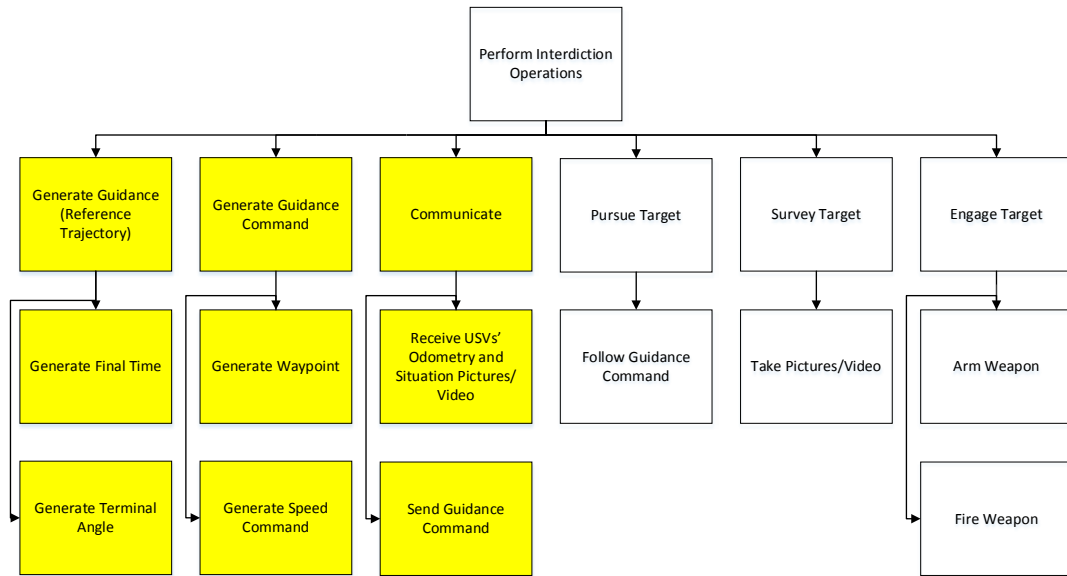


Figure 11. Functional Decomposition of Swarm USVs System.

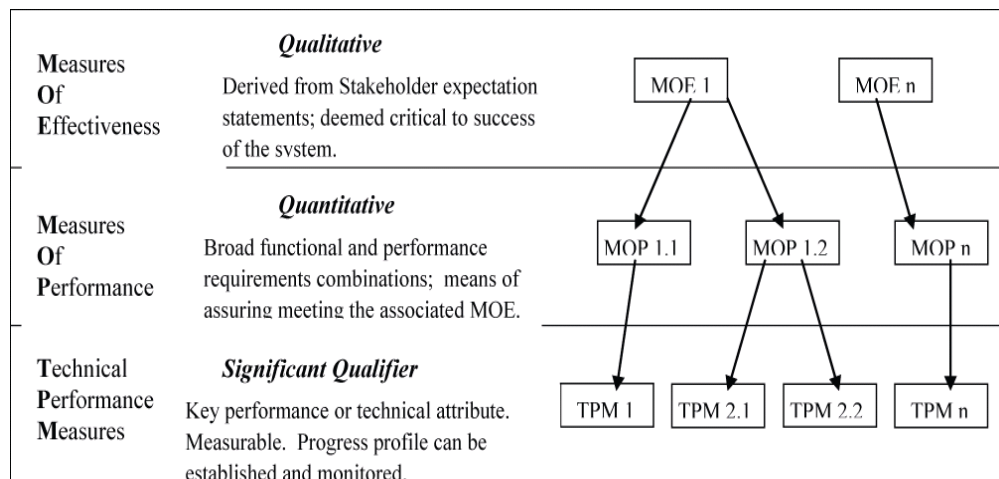


Figure 12. Relationships of MOEs, MOPs, and TPMs.  
Source: Hernandez (2016a).

As driven by the motivation to engage and interdict targets independently or cooperatively with other systems, an appropriate MOE for the system of interest would be the **average number of pursuers required for a successful interdiction**. The corresponding MOP would be **percentage of successful interdictions**. Successful interdictions are dictated by fast computation time and accurate control of the guidance command. Hence, the resulting TPMs would be the **percentage of computation time for guidance generation against the actual mission time** and **percentage of positional and heading error from the predicted intercept point**. These evaluation measures shall be the key design considerations in Chapter III and IV. A summary of the MOE, MOPs, and TPMs, along with objective and descriptions of each, are presented in Table 1.

Table 1. Summary of MOE, MOPs, and TPMs.

No.	Measure of Effectiveness (MOE)	Objective	Description
1	Average number of pursuers required for a successful interdiction	To Minimize	The number of pursuers required is used as a measure of the swarm system's ability to intercept a target with minimal resources.
No.	Measure of Performance (MOP)	Objective	Description
2	Percentage of successful interdictions	To Maximize	This measure reflects the success rate of the swarm system.
No.	Technical Performance Measure (TPM)	Objective	Description
3	Percentage of computation time for guidance generation against the actual mission time	To Minimize	The percentage of computation time for guidance generation against the actual mission time is used to evaluate the computation capability of the system.
4	Percentage of positional and heading errors from the predicted intercept point	To Minimize	The percentage of positional and heading errors from the predicted intercept point is used to evaluate the control capability of the system.

### III. COORDINATED TRAJECTORY-SHAPING GUIDANCE STRATEGY

This chapter was previously published by IEEE (See, Ghosh, and Yakimenko 2017).<sup>1</sup>

Dealing with the problem formulated in Section I.B, the optimal-control-theory-based methods heavily rely on linearized engagement geometry. These methods exhibit a significant sensitivity to time-to-go estimation errors. Sliding-mode-control-based methods and strategies based on proportional navigation (PN) have the potential to explore the problems considering their nonlinearity. However, the advantage of PN-based methods lies in the simple but elegant and efficient user-friendly structure of a guidance command. This chapter begins with the literature review of the previous research on final time and terminal angle control, followed by the formulation of multi-pursuer interdiction problem, and ends with the discussion of strategies for interdiction mission.

#### A. LITERATURE REVIEW

The successful use of a Control Architecture for CARACaS in USVs for overwhelming adversaries has firmly paved the path in this direction for unmanned systems in general (Smalley 2014).

A coordinated trajectory-shaping guidance strategy is developed for a group of unmanned pursuers to this end. Specific challenges lie in achieving a control of arrival time in the form of simultaneous arrival at desired arrival angles relative to the target's final states. Thus, this problem calls for a synchronization of both final time control and terminal angle control.

---

<sup>1</sup> Reprinted with permission from Hongze Alex See, Satadal Ghosh, and Oleg Yakimenko, Towards the Development of an Autonomous Interdiction Capability for Unmanned Aerial Systems, Proceedings of the 2017 International Conference on Unmanned Aircraft Systems (ICUAS), July 2017. This publication is a work of the U.S. Government as defined in Title 17, United States Code, Section 101. Copyright protection is not available for this work in the United States. IEEE will claim and protect its copyright in international jurisdictions where permission from IEEE must be obtained for all other uses, in any current or future media, including reprinting/republishing this material for advertising or promotional purposes, creating new collective works, for resale or redistribution to servers or lists, or reuse of any copyrighted component of this work in other works.

The problems of controlling final time (a.k.a. impact time) and terminal angle (also identified as impact angle) in an engagement have been dealt with mainly in guidance-related literature. Impact angle-constrained engagement problems have been extensively studied using optimal control theory by Kim and Grider (1973), Ohlmeyer (2003), Ryoo, Cho, and Tahk (2006), Shaferman and Shima (2008), Harrison (2012), Cho, Ryoo, Tsourdos, and White (2014) and Bardhan and Ghose (2015); sliding mode control theory by Shima (2011), Rao and Ghose (2013), and Kumar, Rao, and Ghose (2014); and proportional navigation (PN)-based methodology by Kim, Lee, and Han (1998), Ratnoo and Ghose (2008), Ratnoo and Ghose (2010), Lee, Kim, and Tahk (2013), and Ghosh, Ghose, and Raha (2016a); along with and other nonlinear methods like relative circular navigation by Yoon (2008).

The problem of controlling impact time has also been addressed in literature using optimal control theory by Jeon, Lee, and Tahk (2006), and Lee, Jeon, and Tahk (2007); PN-based strategy by Jeon, Lee, and Tahk (2010), and Ghosh, Ghose, and Raha (2013); and sliding mode control theory by Kumar and Ghose (2015). It should be noted that in literature these two problems mostly have been dealt with separately, with the exception of Lee, Jeon, and Tahk (2007), Harrison (2012), and Kumar and Ghose (2015).

However, as mentioned earlier, both arrival angle and arrival time need to be achieved simultaneously for a successful interdiction mission control. This thesis makes a pertinent contribution in this context.

## **B. MULTI-PURSUER INTERDICTION PROBLEM FORMULATION**

### **1. Basic Engagement Configuration**

This thesis considers a planar engagement when pursuers are relatively close to each other but could have different speeds and headings (Figure 13). Pursuers are assumed to be homogeneous with typically a comparable or slight advantage over the target's speed. The target is assumed to be non-maneuvering but moving with a constant speed and heading. The target is also assumed to adopt a flee-away strategy instead of engaging in a close combat and attempting to out-maneuver pursuers. Relying on its speed, therefore, becomes a priority for the target. Pursuers are assumed to be equipped

with sensors allowing them to detect and track the target's location and heading relative to the pursuers. The problem of decision-making for each individual pursuer to determine its own respective position in the formation is out of the scope of this thesis. Thus, it is assumed that the intercept point (IP) and approach angle for each pursuer in the formation are pre-determined by a centralized mission controller. Figure 13 shows an example of engagement configuration with the final desired configuration achieved when all pursuers arrive at the pre-specified relative locations on the circle around the target with the pre-defined headings simultaneously.

In accordance with the planar engagement geometry depicted in Figure 13, each pursuer P is modeled as a point mass moving with constant speed  $V_p = \|\mathbf{V}_p\|$  approaching a stationary target, T. As a result, kinematic equations of motion for two components of the speed vector,  $V_R$  and  $V_\theta$ , respectively, are expressed in terms of the range between P and T,  $R$ , and corresponding line-of-sight (LoS) angle,  $\theta$ , as

$$V_{R(i)} = \dot{R}_{(i)} = -V_{P(i)} \cos(\alpha_{P(i)} - \theta_{(i)}) \quad (1)$$

$$V_{\theta(i)} = R_{(i)} \dot{\theta}_{(i)} = -V_{P(i)} \sin(\alpha_{P(i)} - \theta_{(i)}) . \quad (2)$$

In these equations, “i” represents the  $i$ -th pursuer, and the change of the pursuer's velocity heading angle  $\alpha_p$  is defined by its lateral acceleration  $a_p = \|\mathbf{a}_p\|$  ( $\mathbf{a}_p$  is orthogonal to the speed vector since we consider the case when  $V_p = \text{const}$ ).

$$\dot{\alpha}_{P(i)} = \mathbf{a}_{P(i)} / V_{P(i)} \quad (3)$$

Pursuer's lateral acceleration  $a_p$  is based on the Pure Proportional Navigation (PPN) guidance law with the given by

$$a_{P(i)} = V_{P(i)} \dot{\alpha}_{P(i)} = N_{(i)} V_{P(i)} \dot{\theta}_{(i)} , \quad (4)$$

where  $N$  is the navigation gain.

The problem of having a moving target, as opposed to a stationary target considered in Ghosh et al. (2017) *Unmanned Aerial Vehicle Guidance for an All-Aspect*

*Approach to a Stationary Point*, is dealt with by estimating Predicted IP (PIP). Other than that, the approach angle control is carried in a similar manner, using the so-called approach angle-constrained guidance laws against a stationary target allowing approaching the target from any direction (i.e.,  $\alpha_{P_f} \in [-\pi, \pi)$ ) (Ghosh et al. 2017).

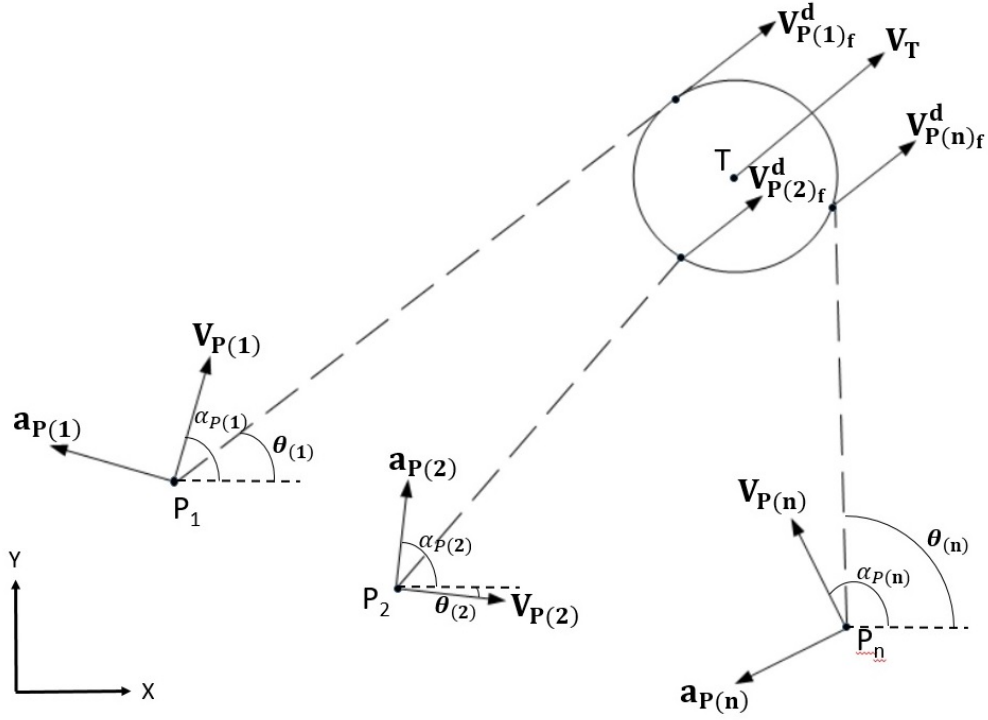


Figure 13. Planar Engagement Geometry.

## 2. Background of PN-based Approach Angle Control

From Equations 3 and 4, the achievable approach angle using the standard PPN guidance is given by

$$\alpha_{P_f} = \alpha_{r_0} + N(\theta_f - \theta_0) . \quad (5)$$

The collision course with a stationary target (PIP in our case) is formed when  $\alpha_{P_f} = \theta_f$  (Dhananjay and Ghose 2014). From Equation 5, it follows that

$$\alpha_{P_f} = (N\theta_0 - \alpha_{r_0}) / (N - 1) . \quad (6)$$

If the condition for the bounded terminal lateral acceleration of pursuer is met ( $N \geq 2$ ), the achievable approach angle interval for  $\alpha_{p_0} \geq \theta_0$ , which is  $\alpha_{p_0} \in [\theta_0, \theta_0 + \pi)$ , using PPN (Shneydor 1998; Ratnoo and Ghose 2010; Ghosh et al. 2017) becomes

$$\alpha_{p_f} \in [2\theta_0 - \alpha_{p_0}, \theta_0), N \geq 2, \quad (7)$$

where  $\alpha_{p_f}$  equals  $2\theta_0 - \alpha_{p_0}$  when  $N = 2$ , and approaches  $\theta_0$  when  $N \rightarrow \infty$ . It could also be noted that using the standard PPN, a significant portion of the angular interval in the halfspace  $[-\pi + \theta_0, \theta_0)$  cannot be achieved since  $[2\theta_0 - \alpha_{p_0}, \theta_0) \subset [-\pi + \theta_0, \theta_0)$ . A two-stage PPN guidance strategy (2pPPN) introduced by Ratnoo and Ghose (2008) expanded the set of the achievable approach angles. Specifically, the following theorem established the achievable approach angle set and corresponding navigation gains for PPN and 2pPPN (Jeon, Lee, and Tahk 2006; Ghosh et al. 2017).

**a. Theorem 1**

In the case of  $\alpha_{p_0} > \theta_0$ , a desired approach angle  $\alpha_{p_f}^d \in [2\theta_0 - \alpha_{p_0}, \theta_0)$  could be attained using PPN with  $N = (\alpha_{p_f}^d - \alpha_p) / (\alpha_{p_f}^d - \theta) \geq 2$ , while  $\alpha_{p_f}^d \in [-\pi + \theta_0, 2\theta_0 - \alpha_{p_0})$  could be achieved using 2pPPN with

$$N = \left\{ \begin{array}{l} \left( \frac{2}{\pi} \right) \{ \alpha_{p_0} - \theta_0 \}; \text{if } (\alpha_{p_f}^d - \alpha_p) / (\alpha_{p_f}^d - \theta) < 2 \\ (\alpha_{p_f}^d - \alpha_p) / (\alpha_{p_f}^d - \theta); \text{if } (\alpha_{p_f}^d - \alpha_p) / (\alpha_{p_f}^d - \theta) \geq 2 \end{array} \right\}. \quad (8)$$

Examples of trajectories utilizing PPN and 2pPPN for  $\alpha_{p_f}^d = -\frac{\pi}{6}$ , and  $\alpha_{p_f}^d = -\frac{5\pi}{6}$ , respectively, with and without the look-angle ( $\mu = \alpha_p - \theta$ ) constraint are presented in Figure 14. It should be noted that the initial range between the pursuer and target should be sufficiently large and is determined by the initial LoS rate, maximum turn rate of pursuer, pursuer's speed, and desired terminal angle. Following a similar methodology for  $\alpha_{p_0} \in (-\pi + \theta_0, \theta_0)$  Theorem 1 can be restated as shown in Observation 1.

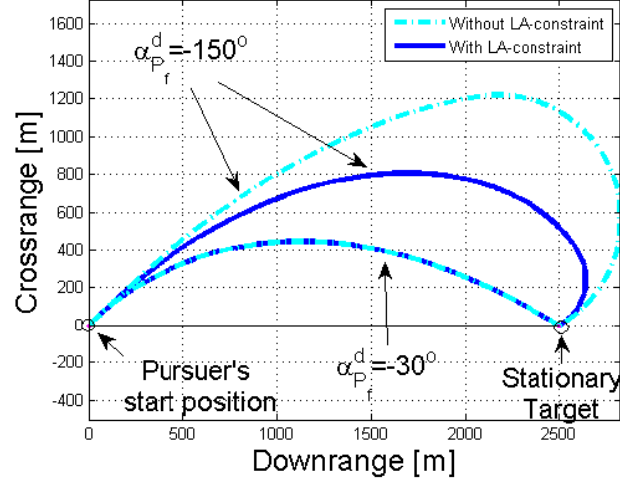


Figure 14. Examples of Pursuer Trajectory for PPN and 2pPPN.  
Source: Ghosh et al. (2017).

**b. Observation 1**

In the case of  $\alpha_{P_0} < \theta_0$ , a desired approach angle  $\alpha_{P_f}^d \in (\theta_0, 2\theta_0 - \alpha_{P_0}]$  could be attained using PPN with  $N = (\alpha_{P_f}^d - \alpha_P) / (\alpha_{P_f}^d - \theta) \geq 2$ , while  $\alpha_{P_f}^d \in (2\theta_0 - \alpha_{P_0}, \pi + \theta_0]$  could be achieved by 2pPPN with

$$N = \left\{ \begin{array}{l} \left( \frac{2}{\pi} \right) |\alpha_{P_0} - \theta_0|; \text{if } (\alpha_{P_f}^d - \alpha_P) / (\alpha_{P_f}^d - \theta) < 2 \\ (\alpha_{P_f}^d - \alpha_P) / (\alpha_{P_f}^d - \theta); \text{if } (\alpha_{P_f}^d - \alpha_P) / (\alpha_{P_f}^d - \theta) \geq 2 \end{array} \right\}. \quad (9)$$

Since for two specific initial conditions (collision course  $\alpha_{P_0} = \theta_0$  and inverse collision course  $\alpha_{P_0} = -\pi + \theta_0$ ) algorithm cannot start, use of an adjustment bias was suggested (Ghosh et al. 2017).

The approach angle control considered in this thesis is an extension over the results in Theorem 1 and Observation 1 stated above to accommodate the requirement of simultaneous arrival of pursuers at the desired final intercept points relative to now moving target.

### 3. Background of PN-based Final Time Control

As mentioned above, a PIP needs to be computed with respect to the target's estimated position and heading. For that, time-to-go should be computed for each pursuer in the group. A closed-form time-to-go estimate for the stationary targets is given by

$$\hat{t}_{go} = \left\{ \begin{array}{l} \left( \frac{R}{V_p} \right) \left\{ 1 + \frac{\theta_p^2}{[2(2N-3)]} \right\}; \text{if } \left( N > \frac{3}{2} \right) \\ \left( \frac{R}{V_p} \right) \left[ 1 - 2\theta_p^2 \left\{ 1 - \frac{\left[ \ln \left( \frac{R}{R_{\min}} \right) \right]}{4} \right\} \right]; \text{if } \left( N = \frac{3}{2} \right) \end{array} \right\}, \quad (10)$$

where  $R_{\min}$  represents the minimum range for an intercept to occur. More details of this result can be found in Ghosh, Ghose, and Raha (2016b) *Unified Time-To-Go Algorithms for Proportional Navigation Class of Guidance*. This approximate form of time-to-go is dependent on instantaneous range  $R$ , angle between pursuer heading and LoS  $\theta_p$  (known as heading error with respect to the target), navigation gain  $N$ , and pursuer's speed.

As PIPs are computed for all pursuers, and corresponding time-to-go estimates are obtained, this information could be utilized for adaptive variation of navigation gain of some of the pursuers. The next section specifically addresses strategies and algorithms for a two-pursuer intercept model.

## C. STRATEGIES FOR INTERDICTION MISSION

### 1. PIP Estimation for Each Pursuer

The first step to achieve simultaneous arrival time for all pursuers is to estimate the time-to-go for each pursuer to their respective PIP,  $\hat{t}_{go(i)}$ . The algorithm to estimate the time-to-go for each control cycle is as follows:

- (1) Initialization step (at the start of every control cycle)
- (a) Obtain information about the current range  $R_{mag(i)} = \|\mathbf{R}_{mag(i)}\|$  from the target, velocity  $V_{P(i)}$  and current heading  $\alpha_{P(i)}$  for Pursuers 1 and 2, together with the speed of the target  $V_T = \|\mathbf{V}_T\|$  and target's current heading,  $\alpha_T$ .
- (b) Guess the time-to-go  $t_{guess(i)}$  for each pursuer

$$t_{guess(i)} = \frac{1}{2} \left( \frac{R_{mag(i)}}{V_{P(i)} - V_T} + \frac{R_{mag(i)}}{V_{P(i)} + V_T} \right). \quad (11)$$

- (2) Recursion step (within a control cycle). Follow this step while the difference between  $t_{guess(i)}$  and  $\hat{t}_{go(i)}$  is less than 5% (i.e.,  $t_{guess(i)} \geq 1.05\hat{t}_{go(i)}$ ) or  $t_{guess(i)} \leq 0.95\hat{t}_{go(i)}$ . Otherwise, go to Step 3.

- (a) Use  $t_{guess(i)}$  to compute the coordinates of the guessed PIP  $\hat{\mathbf{R}}_{guess(i)}$  from the guessed time-to-go value,  $t_{guess(i)}$ , with the current desired PIP  $\mathbf{R}(i)$  for each individual pursuer

$$\hat{\mathbf{R}}_{guess(i)} = \mathbf{R}(i) + \mathbf{V}_T t_{guess(i)}. \quad (12)$$

- (b) Obtain the LoS angle  $\theta_{guess(i)}$  for Pursuers 1 and 2 with respect to (w.r.t.) guessed PIP, to compute the required navigation gain for each pursuer

$$N_{(i)} = \left( \alpha_T - \alpha_{P(i)} \right) / \left( \alpha_T - \theta_{guess(i)} \right). \quad (13)$$

- (c) Following Equation 10 evaluate the time-to-go estimate  $\hat{t}_{go(i)}$  for each pursuer with parameters  $\hat{R}_{guess(i)} = \|\hat{\mathbf{R}}_{guess(i)}\|$ ,  $V_{P(i)}$ ,  $\theta_{P(i)} = \alpha_{P(i)} - \theta_{guess(i)}$  and  $N_{(i)}$ .

- (d) Increase or decrease the guessed time-to-go  $t_{guess(i)}$  with a half the difference between  $t_{guess(i)}$  and time-to-go estimate  $\hat{t}_{go(i)}$

$$t_{guess(i)} = t_{guess(i)} + \left( \hat{t}_{go(i)} - t_{guess(i)} \right) / 2 . \quad (14)$$

- (3) Exit step. The time-to-go estimate for each pursuer  $\hat{t}_{go(i)}$  to the PIP is obtained for the control cycle. And, the PIP, LoS angle and gain for the control cycle is obtained as,

$$\begin{aligned} \mathbf{R}_{PIP(i)} &= \mathbf{R}(i) + \mathbf{V}_T \hat{t}_{go(i)} ; \left( \theta_{(i)} = \theta_{guess(i)} \right) \\ N_{(i)} &= \left( \alpha_T - \alpha_{P(i)} \right) / \left( \alpha_T - \theta_{(i)} \right) \end{aligned} . \quad (15)$$

## 2. Trajectory-Shaping Strategy for Multiple Pursuers

In the guidance generation, the moving target is computed as a stationary target in every computational cycle (sometimes called the control cycle). Therefore, the overall guidance algorithm could be adopted from Theorem 1 and Observation 1, where “a proportional navigation-based guidance law is proposed for capturing all possible impact angles in a surface-to-surface planar engagement against a stationary target” (Ratnoo and Ghose 2008, 1816).

Following Theorem 1 and Observation 1, angle control is achieved. However, to implement final time control, a further adaptive modulation of navigation gain is required, which is discussed next.

According to Equation 10, in order to enable a synchronized arrival of all pursuers, they should adjust either their speed profiles or navigation gains. Reducing the navigation gain of pursuer with a lower time-to-go to a value less than 2, allows the pursuer to travel a longer trajectory and acts as a kind of an extra roaming phase for the corresponding pursuer. The navigation gain value greater than or equal to 1 also ensures that the target and PIP are still within its field of view. A computation procedure for the two-pursuer case looks like the following:

(1) Initialization step. The time-to-go estimates  $\hat{t}_{go(1)}$  and  $\hat{t}_{go(2)}$ , and corresponding navigation gains,  $N_{(1)}$  and  $N_{(2)}$ , at each control cycle for Pursuers 1 and 2 are obtained from Step 3 of PIP estimation algorithm in Section C.1.

(2) If  $\left( \left| \hat{t}_{go(1)} - \hat{t}_{go(2)} \right| \leq \underline{t}_{go_h} \right)$ , the navigation gains  $N_{(1)}$  and  $N_{(2)}$  for Pursuers 1 and 2 remain unchanged.

(3) Recursive step (over control cycles). While  $\left( \left| \hat{t}_{go(1)} - \hat{t}_{go(2)} \right| \geq \underline{t}_{go_h} \right)$ , set  $N_{(1)} = 1$  if  $\hat{t}_{go(2)} > \hat{t}_{go(1)}$  or  $N_{(2)} = 1$  if  $\hat{t}_{go(1)} > \hat{t}_{go(2)}$ . Compute the new positions for the next control cycle of Pursuers 1 and 2 with  $N_{(1)}$  and  $N_{(2)}$ , respectively, and thus for the next control cycle  $\hat{t}_{go(1)}$  and  $\hat{t}_{go(2)}$  till  $\left( \left| \hat{t}_{go(1)} - \hat{t}_{go(2)} \right| \leq \underline{t}_{go_h} \right)$ . Go to Step 4.

(4) Recursive step (over control cycles). While  $\left( \left| \theta_{(1)} - \alpha_T \right| \geq \frac{\pi}{12} \right)$  re-initiate gain scheduling for pursuer 1 by setting  $N_{(1)} = 1$  if  $\left( \left| \hat{t}_{go(2)} - \hat{t}_{go(1)} \right| \geq \bar{t}_{go_h} \right)$ , and while  $\left( \left| \theta_{(2)} - \alpha_T \right| \geq \frac{\pi}{12} \right)$  re-initiate gain scheduling for pursuer 2 by setting  $N_{(2)} = 1$  if  $\left( \left| \hat{t}_{go(1)} - \hat{t}_{go(2)} \right| \geq \bar{t}_{go_h} \right)$ . For each successive control cycle repeat this gain scheduling for pursuer 1 until  $\left( \left| \theta_{(1)} - \alpha_T \right| < \frac{\pi}{12} \right)$  or  $\left( \left| \hat{t}_{go(1)} - \hat{t}_{go(2)} \right| \leq \underline{t}_{go_h} \right)$ , and for pursuer 2 until  $\left( \left| \theta_{(2)} - \alpha_T \right| < \frac{\pi}{12} \right)$  or  $\left( \left| \hat{t}_{go(1)} - \hat{t}_{go(2)} \right| \leq \underline{t}_{go_h} \right)$ .

(5) Recursive step (over control cycles). Otherwise use  $N_{(1)}$  and  $N_{(2)}$  computed from Step 3 of PIP estimation algorithm in section C.1. until pursuers arrive at their corresponding PIPs.

In this thesis, the threshold of  $\bar{t}_{go_h} = 3s$  has been considered as different from the threshold of  $\underline{t}_{go_h} = 1s$  used in Step 2 and Step 3. In Step 2 and 3, an attempt is made to bring Pursuers 1 and 2 to arrive simultaneously within the considered  $\underline{t}_{go_h} = 1s$  for the first time. Following this, no gain scheduling is performed and the positions of the

pursuers are computed along with the computed  $N_{(1)}$  and  $N_{(2)}$ . During this time the difference in  $\hat{t}_{go(i)}$  is likely to grow. Attempts to reduce the difference in  $\hat{t}_{go(i)}$  are made again when the difference grew to the threshold of  $\bar{t}_{go_{th}} = 3\text{s}$ .

### 3. Simulation Results

This section presents and discusses the results of two simulations characterizing two different intercept scenarios. In all simulations the integration step (a.k.a. control cycle) was 0.05s (corresponding to the 20-Hz update rate). All simulations were executed on an Intel Core i7 2.20 GHz computer with 8.00 GB RAM in the MATLAB development environment.

The simulations have the following similar engagement parameters: initial coordinates of Pursuer 1  $\mathbf{R}_{p_1} = [0, 0]^T$  m, initial coordinates of Pursuer 2  $\mathbf{R}_{p_2} = [0, 0]^T$  m, initial coordinates of non-maneuvering moving target  $\mathbf{R}_T = [2500, -1000]^T$  m, final desired angle of Pursuer 1 intercept point with respect to target's heading  $\theta_{p_1-T} = \frac{\pi}{4}$ , final desired angle of Pursuer 2 intercept point with respect to target's heading  $\theta_{p_2-T} = -\frac{3\pi}{4}$ , final desired range of Pursuer 1 intercept point from target  $R_{p_1-T} = 100\text{m}$  and final desired range of Pursuer 2 intercept point from target  $R_{p_2-T} = 100\text{m}$ . The two pursuers in each simulation will have a different initial heading. The two pursuers in different simulations may have either the same or different speeds. For simulation with same velocity magnitude, the initial velocity vector of Pursuer 1  $\mathbf{V}_{p_1} = 50 * \left[ \cos\left(\frac{2\pi}{3}\right), \sin\left(\frac{2\pi}{3}\right) \right]^T$  m/s and the initial velocity vector of Pursuer 2  $\mathbf{V}_{p_2} = 50 * \left[ \cos\left(\frac{3\pi}{4}\right), \sin\left(\frac{3\pi}{4}\right) \right]^T$  m/s. For simulation with different speed magnitudes,

the initial velocity vector of Pursuer 1  $\mathbf{V}_{p_1} = [-35, 25]^T$  m/s and the initial velocity vector of Pursuer 2  $\mathbf{V}_{p_2} = [-40, 30]^T$  m/s.

To begin with, Figures 15 (Case 1) and 16 (Case 2) represent trajectories of two pursuers approaching a stationary target. The idea is to demonstrate/reiterate that simulations involving non-maneuvering target are a product of considering the target to be stationary at every computational cycle. Case 1 shows the simulation when the two pursuers have the same speed. Case 2 shows the simulation when the two pursuers have different speeds.

In Figures 17a and 18a are demonstrated the convergence of the approach simultaneously with the time histories of the navigation gain of pursuers and time histories of the angle between pursuers and LoS for Case 1 and Case 2, respectively. Figures 17b and 18b further demonstrate the convergence of the approach with the range between pursuers and the intercept points and the distance between the pursuers converging toward 200m, which is the absolute distance between the pursuers based on  $R_{p_1-T}$  and  $R_{p_2-T}$ . It also demonstrates that there is no collision between the pursuers during the approach. In Figures 15, 16 and 19 (Cases 3–5), the control cycle that a pursuer has been assigned the navigation gain value of 1 is marked in black and labeled “gain scheduling.”

In Figure 19 are simulation results similar to those of Figures 15 and 16, with the exception of a non-maneuvering moving target instead of a stationary target in three different cases. Case 3 shows the simulation when two pursuers have the same speed to a non-maneuvering target with velocity vector  $\mathbf{V}_T = [0, -20]^T$  m/s. Case 4 shows the simulation when two pursuers have different speeds to a non-maneuvering target with velocity vector  $\mathbf{V}_T = [0, -20]^T$  m/s. Case 5 shows the simulation when two pursuers have the same speed to a non-maneuvering target with velocity vector  $\mathbf{V}_T = [-20, -20]^T$  m/s.

The range to the intercept point graphs in Figures 20–22 demonstrate the concept of simultaneous approach with the convergence of the pursuers at their respective

intercept points at the end of the guidance computation. While the aim of the guidance strategy is set up to achieve pinpoint simultaneous approach for both pursuers, it is noticed that the ranges of both pursuers did not fully converge. This phenomenon can be seen in the distance between pursuers graph in Figures 17, 18 and 20–22, where the end distance between both pursuers are not exactly 200m. This phenomenon is further illustrated in the range to intercept graph in Figure 22b, where Pursuer 1 (represented by the pink line) has yet to arrive at its intercept point. This observation is expected and will vary with different threshold limits stated in Section I.B. It can also be observed in Figures 15, 16, and 19 that the pursuer that is scheduled a navigation gain value of 1 took a longer path at that particular section while the corresponding pursuer caught up, seen in navigation gain graphs and the range to intercept point graphs in Figures 17, 18, and 20–22.

The time history of the heading error with respect to the target shown in Figures 17, 18, and 20–22, demonstrates that the angle between the pursuers' heading and LoS and demonstrate the angle-constrained approach where the heading errors of the pursuers converged to zero (aligned with the LoS) at the end of the guidance computation. In this simulation, it was pre-determined that the final desired pursuers' headings will be similar to the target's heading.

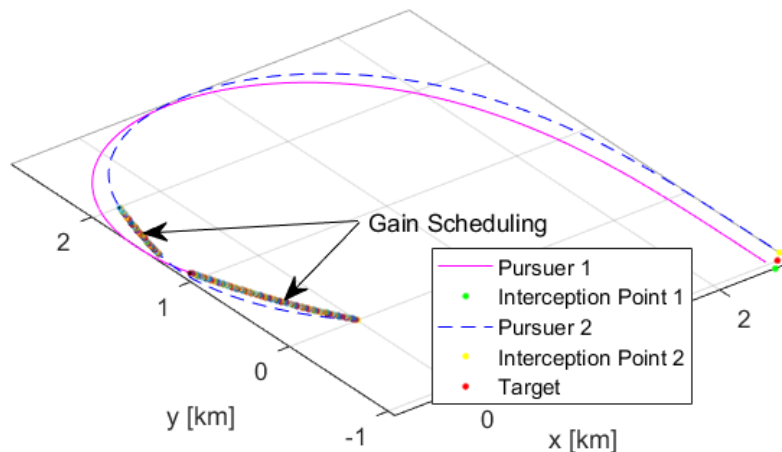


Figure 15. Trajectories of Two Pursuers with the Same Speed to a Stationary Target (Case 1).

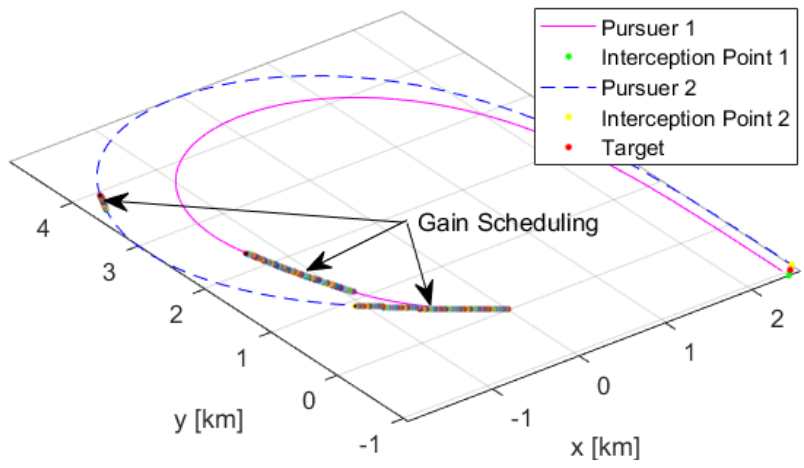
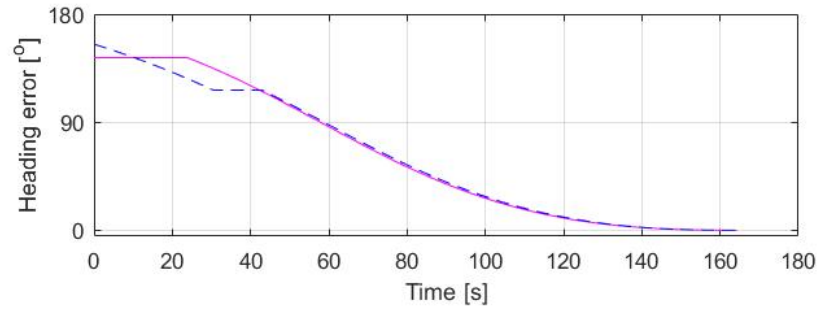
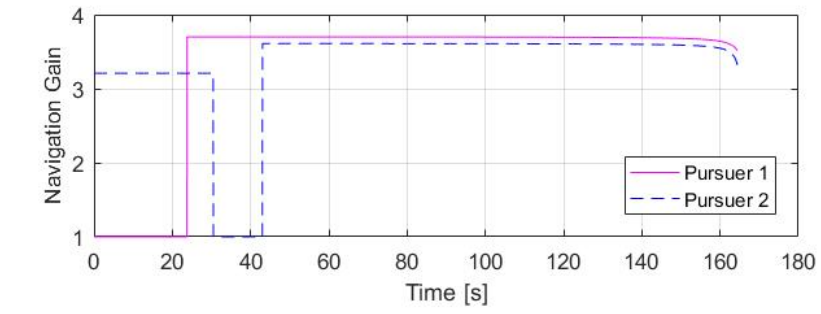
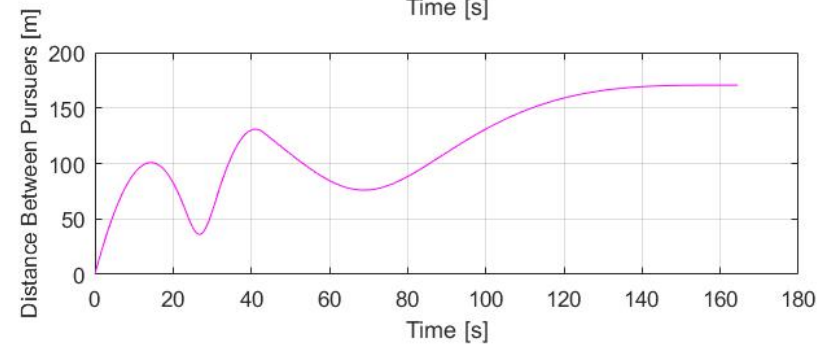
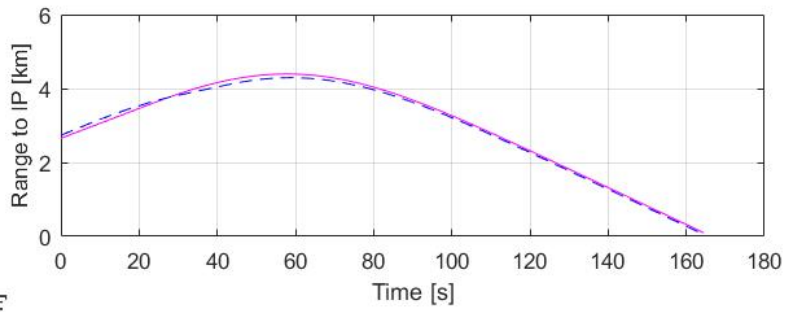


Figure 16. Trajectories of Two Pursuers with Different Speeds to a Stationary Target (Case 2).

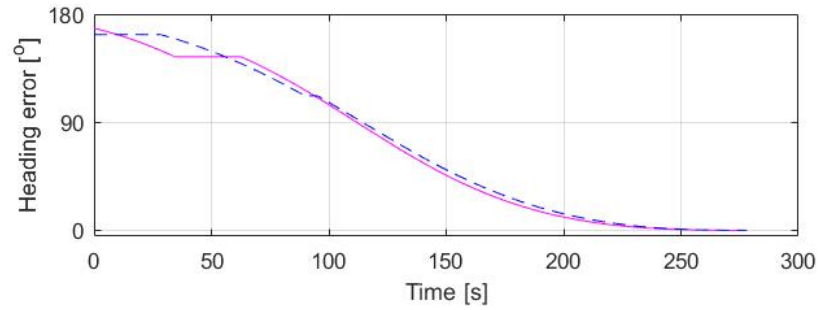
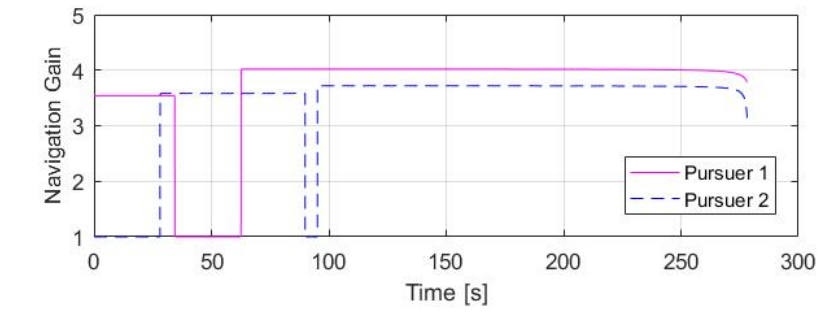


a)

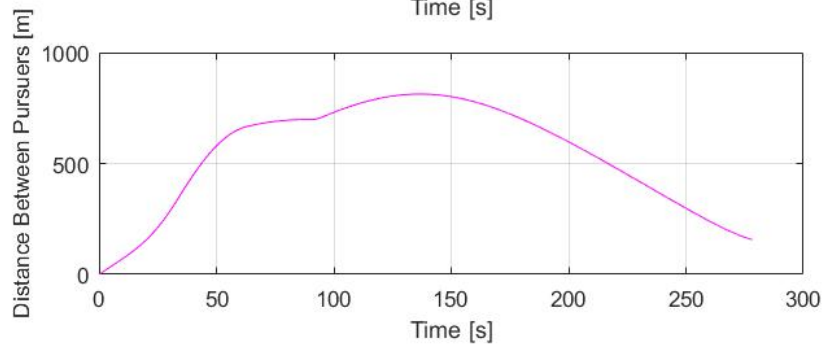
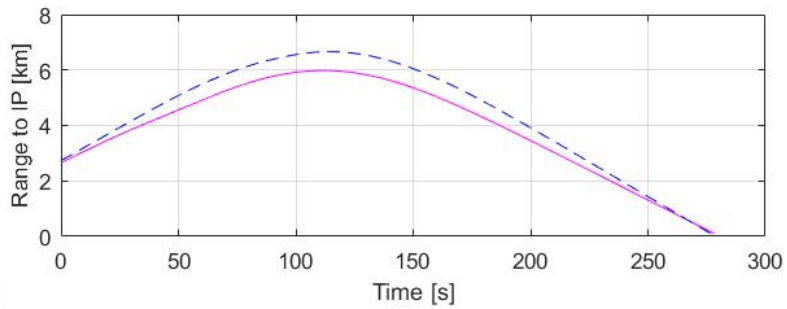


b)

Figure 17. Intercept Characteristics for Two Pursuers for Case 1.



a)



b)

Figure 18. Intercept Characteristics for Two Pursuers for Case 2.

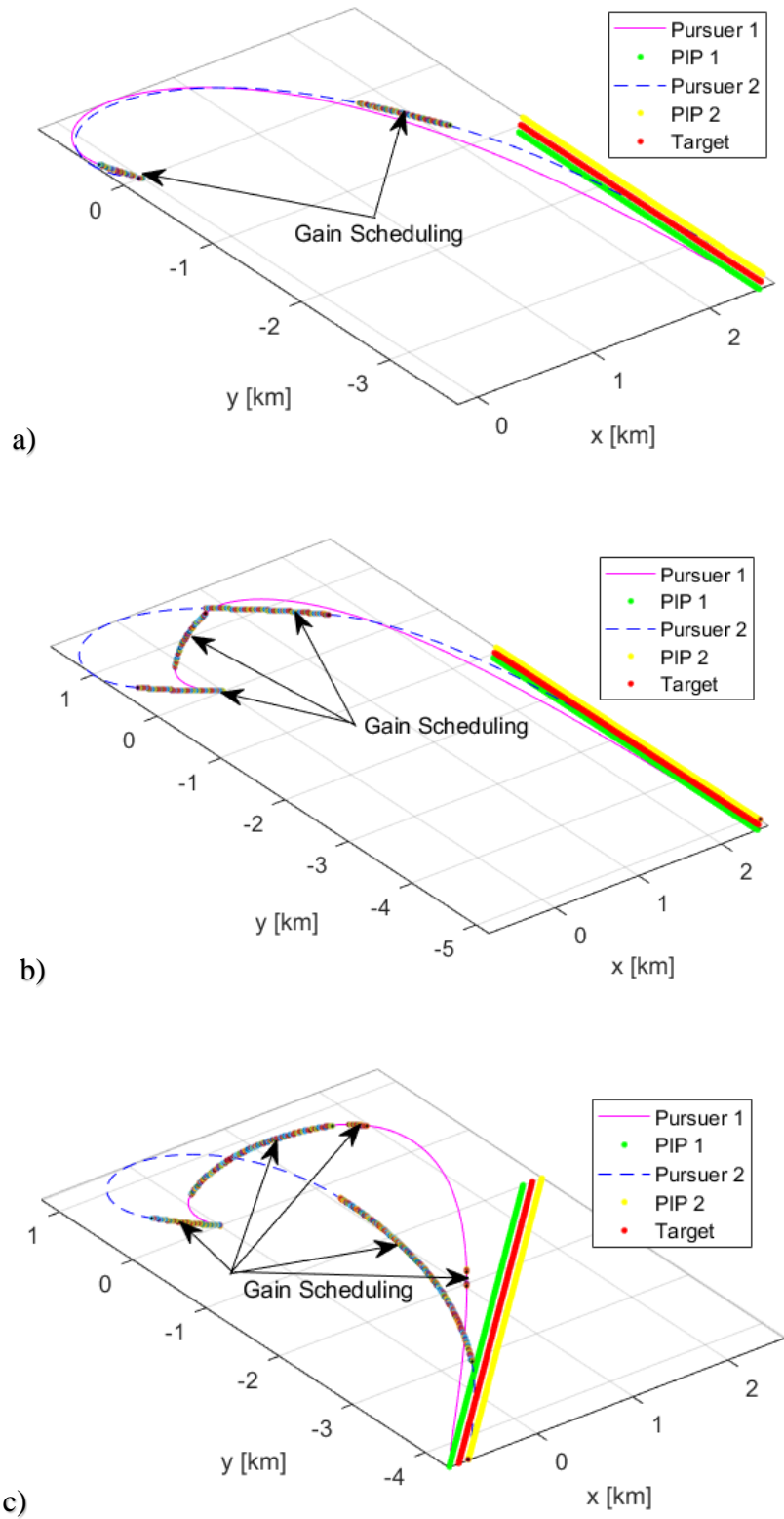
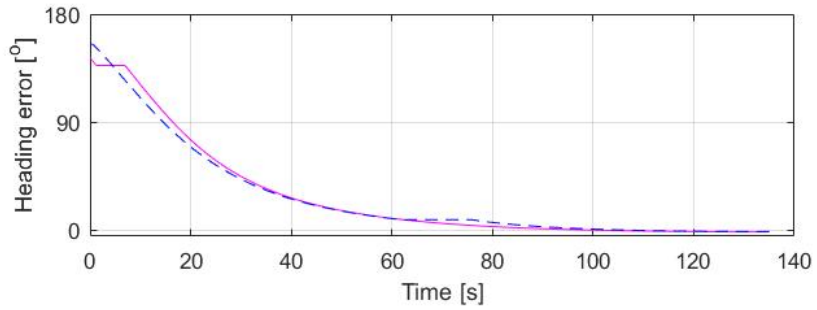
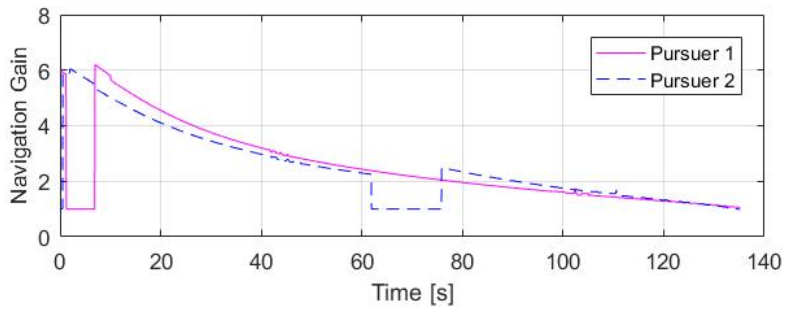
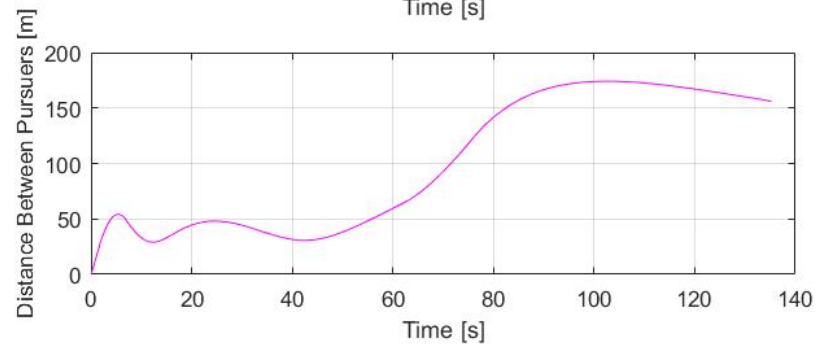
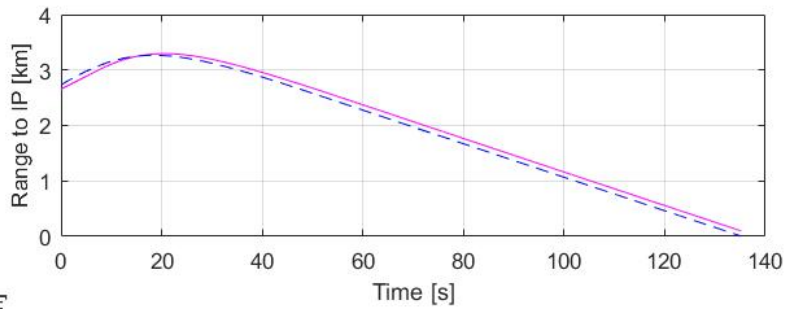


Figure 19. Trajectories of Two Pursuers to a Non-maneuvering Target (Cases 3–5).

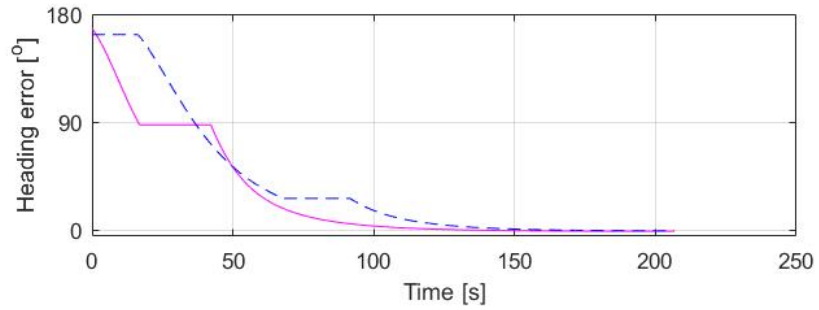
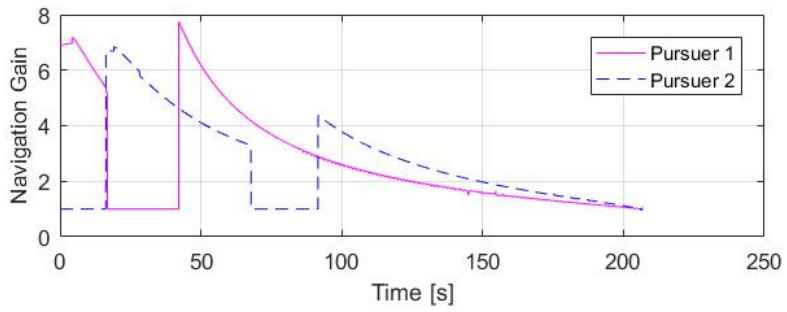


a)

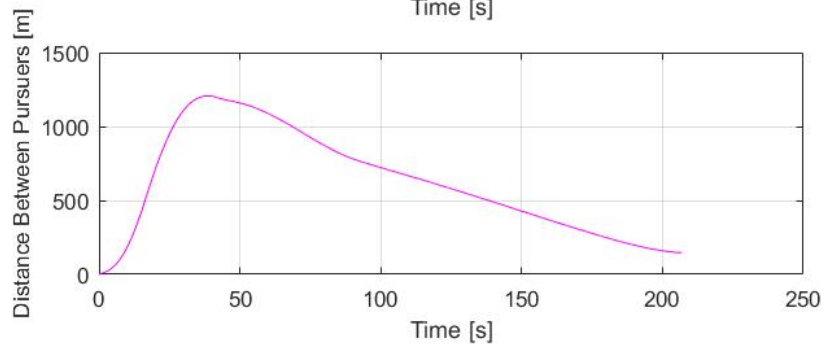
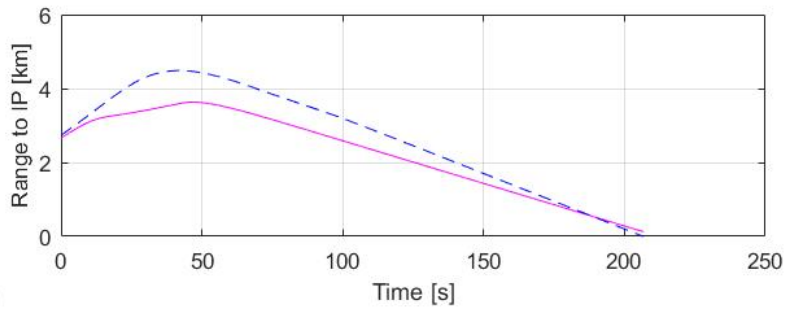


b)

Figure 20. Intercept Characteristics for Two Pursuers for Case 3.

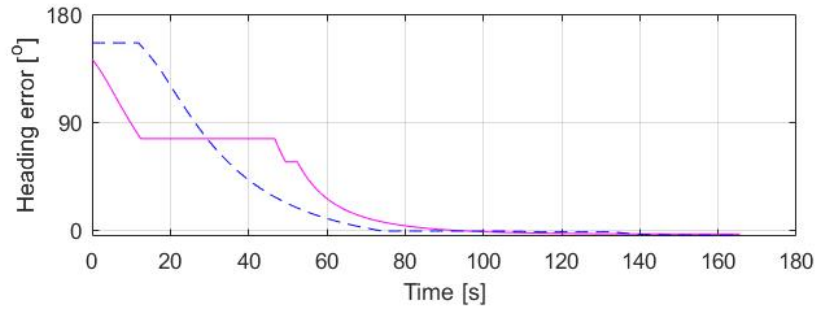
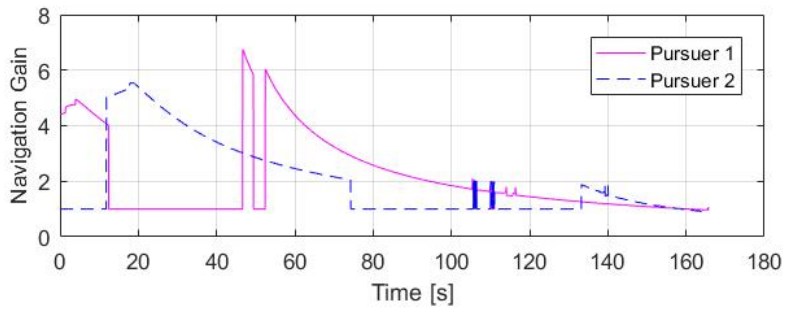


a)

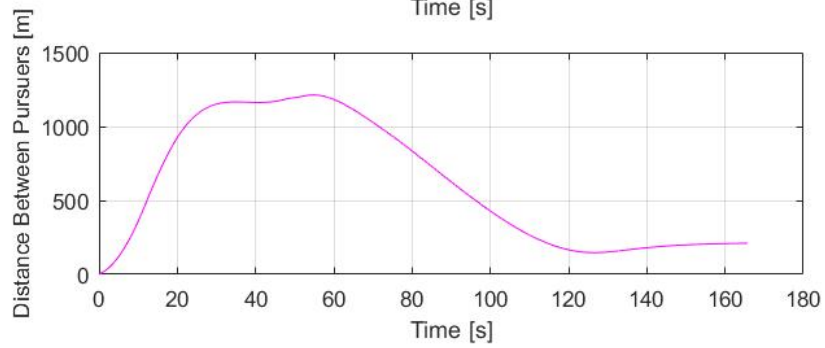
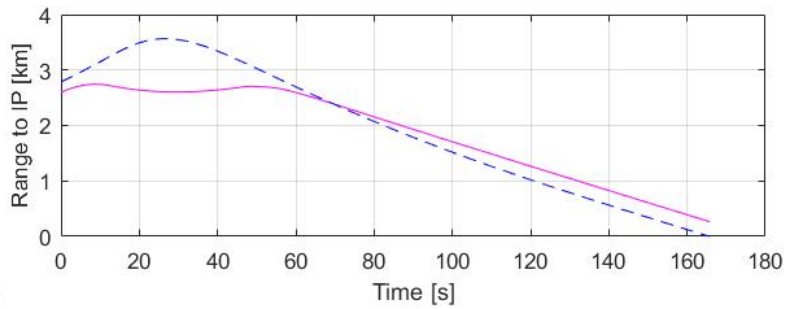


b)

Figure 21. Intercept Characteristics for Two Pursuers for Case 4.



a)



b)

Figure 22. Intercept Characteristics for Two Pursuers for Case 5.

#### 4. Discussion of Simulation Results

As mentioned at the start of Section III.C.3, these simulations were conducted in the MATLAB development environment. The total guidance computation time with its respective mission time for each simulation is presented in Table 2. As seen even using interpretative execution instructions (not compiled code), the executing time requires less than 3% of the duration of a maneuver. As known, compiled code runs about 100 times faster (i.e., it will take less than 0.1s to produce a solution) (Yakimenko 2000). This implies that the algorithm can be run in real-time implementation.

Table 2. Computation Time vs. Mission Time.

Scenario	Computation Time (s)	Mission Time (s)	Ratio (%)
Figure 15	< 5	≈ 165	3.00
Figure 16	< 8	≈ 280	2.86
Figure 19a	< 4	≈ 135	2.96
Figure 19b	< 6	≈ 200	3.00
Figure 19c	< 5	≈ 165	3.00

THIS PAGE INTENTIONALLY LEFT BLANK

## **IV. CODE IMPLEMENTATION IN HIGH-FIDELITY SIMULATION ENVIRONMENT**

With the development of the coordinated trajectory-shaping guidance strategy in Chapter III, the next question is to consider the optimal interval for a guidance command when the algorithm is implemented onboard of a real USV. An optimal guidance command interval aims to reduce the computation burden either onboard the USVs or the command ship and yet, allows the USVs to travel a trajectory that is comparable to the reference trajectory within acceptable tolerances. This chapter begins with the tools and methodology for setting up the simulation environment, followed by a study and discussion on the effects of different guidance command interval while implementing the developed algorithms on an onboard autopilot, using high-fidelity simulation environment.

### **A. SIMULATION SOFTWARE**

All simulations discussed in this chapter were conducted using Gazebo simulation environment. According to Gazebo (2016),

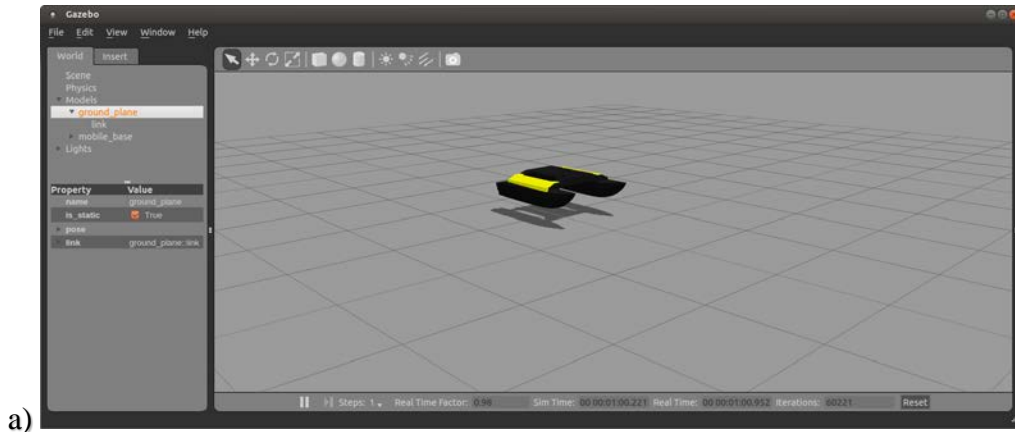
Gazebo is a 3D dynamic simulator with the ability to accurately and efficiently simulate populations of robots in complex indoor and outdoor environments. While similar to game engines, Gazebo offers physics simulation at a much higher degree of fidelity, a suite of sensors, and interfaces for both users and programs. Typical uses of Gazebo include: 1) testing robotics algorithms, 2) designing robots, and 3) performing regression testing with realistic scenarios. (Gazebo 2016)

Gazebo offers a high level of customization for various scenarios, for example, adding robots and with options of different sensors such as inertial measurement unit (IMU), global positioning system (GPS), and cameras, obstacles and objects to model a system as close as possible to real life environment. This allows evaluation and testing of the robots in challenging scenarios without any risk to the actual robots. Even illumination, gravity and inertial in the simulated world can be changed as required. The modelling of the system is achieved by a few steps. The first step would be to create the main file, which is the launch file. The launch file declares the number of robots, along

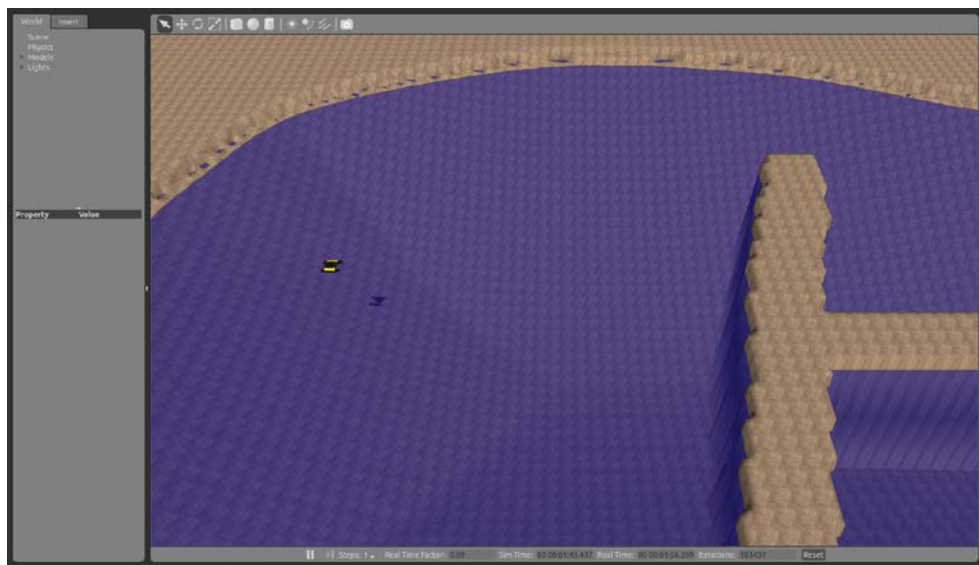
with their spawn positions and their initial headings. The launch file also contains directories of other files, which are essential for the simulation. For example, the Universal Robotic Description Format (URDF) file describes the elements of the robots. Another example would be the world file, which shapes the simulated world visually where terrains, obstacles and other objects are defined. By launching the launch file, Gazebo loads the defined system and starts Gazebo client. An example of an actual ROS-enabled USV (Clearpath Robotics Kingfisher) is shown in Figure 23 and the corresponding model in different simulated worlds is shown in Figure 24.



Figure 23. Clearpath Robotics Kingfisher USV.  
Source: Unmanned Systems Technology (2014).



a)



b)

Figure 24. Gazebo Client (Simulation of Kingfisher USV in Different Worlds).  
Source: NPS Wiki (2017).

## B. MODEL INTERFACES

USV model for this chapter was developed using MathWorks Simulink. This model interfaced with Gazebo simulation environment over the ROS network as ROS nodes. The open-source ROS is a meta-operating system for robots (ROS Wiki 2014). It is also a “flexible framework for writing robot software” with a “collection of tools, libraries, and conventions that aim to simplify the task of creating complex and robust

robot behavior across a wide variety of robotic platforms” (ROS 2013b). It provides the “services expected from an operating system, including hardware abstraction, low-level device control, implementation of commonly-used functionality, message-passing between processes, and package management” (ROS Wiki 2014), along with “high-level functionalities such as asynchronous and synchronous calls, centralized database, a robot configuration system” (Generation Robots 2016). Some “robot-specific capabilities that ROS provides are: 1) standard message definitions for robots, 2) robot geometry library, 3) robot description language, 4) pre-emptible remote procedure calls, 5) diagnostics, 6) pose estimation, 7) localization, 8) mapping and 9) navigation” (ROS 2013a). As explained in MathWorks (2015) webpage,

The primary mechanism for ROS nodes to exchange data is to send and receive messages. Messages are transmitted on a topic and each topic has a unique name in the ROS network. If a node wants to share information, it will use a publisher to send data to a topic. A node that wants to receive that information will use a subscriber to that same topic. Besides its unique name, each topic also has a message type, which determines the types of messages that are allowed to be transmitted. (MathWorks 2015)

Figure 25 illustrates the concept of topics, messages, publishers and subscribers.

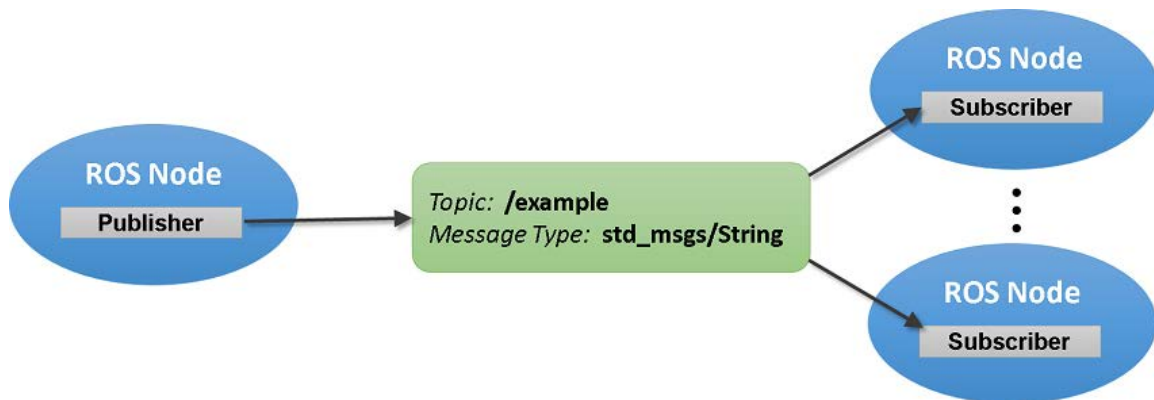


Figure 25. Concept of Data Exchange in ROS. Source: MathWorks (2015).

The “RQT graph” in Figure 26 further illustrates the concept shown in Figure 25 with the actual data exchange between the ROS nodes in the simulation environment. The ROS node, KingFisher\_54689 (Simulink Model), subscribes to the “/imu/data” topic and receives messages containing the current poses of the robots in the simulation. These pose messages are published by Gazebo through the same topic. The Simulink node generates guidance commands as “drive” messages based on the received robots’ poses and publishes them to the “/cmd\_drive” topic. Gazebo subscribes to the “/cmd\_drive” topic and receives the “drive” messages, which command the robots to move in the simulation.

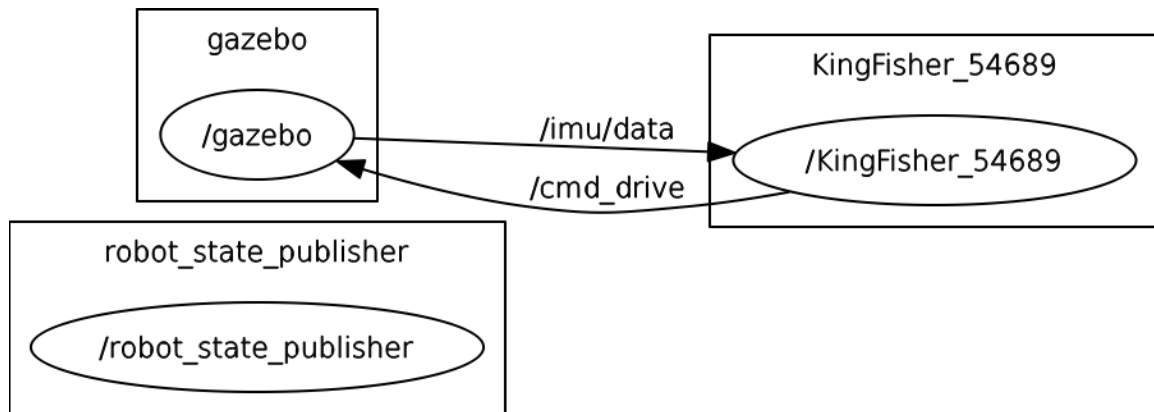


Figure 26. Data Exchange between ROS Nodes during the Simulation.

### C. TEST AND EVALUATION

The objective of the simulation and study shall be explained first to allow better understanding of the methodology in achieving them. As stated at the start of this chapter, the objective is to determine the optimal interval for guidance command. An optimal guidance command interval aims to reduce the computation burden either onboard the USVs or the command ship and yet, allows the USVs to travel a trajectory that is comparable to the reference trajectory within acceptable tolerances. Figure 27 illustrates the effects of different guidance command intervals on the actual trajectories travelled by

the USV in two distinct intervals. Figure 27a demonstrated a case of short guidance command interval and hence, the close proximity between waypoints. The actual trajectory travelled by the USV is represented by the black solid line, and it can be observed that the travelled trajectory matches the reference trajectory (computed strategy) to a large extent. Figure 27b demonstrated a case of large guidance command interval, which is apparent in the distance between the various waypoints. The resulting travelled trajectory does not match the reference trajectory as well as with the case of small guidance command interval, especially at the beginning where the gradient of the curve is steeper. Significantly, the illustrations in Figure 27 have the assumption that the USV is controlled only by a waypoint controller with no proportional integral derivative (PID) controller in place, resulting in only straight path between waypoints.

The reference trajectory in Figure 27, represented by the pink solid line, shall be the reference trajectory for the USVs in the simulations. This reference trajectory is deemed suitable for our study due to the mixture of curve gradients. It is noticeable that the initial portion of the trajectory has a steeper curve than the later portion, which allows a better study on the effects of different guidance command intervals, specifically on curvy trajectories. It took a total of 461 control cycles to generate the reference trajectory. Recall that the integration step (control cycle) was 0.05s (corresponding to the 20-Hz update rate) as stated in Section III.C. Each control cycle in the guidance generation determines the next position and heading that the USV will be in. However, it is impractical to translate every guidance generation to guidance command for each control cycle, which would create an unnecessary computation burden on the USV or command ship onboard computers. Therefore, the guidance command intervals that were selected for the study ranged from approximately 5% to approximately 30% of the total guidance generation control cycles. The guidance command intervals that were tested, the number of control cycles in relation to the intervals, and the total number of waypoints as a result of the intervals in the simulation are shown in Table 3.

Table 3. Guidance Command Intervals Tested.

Guidance Command Intervals (s)	Number of Control Cycles	Number of Waypoints
1	20	24
2.5	50	10
4	80	6
5	100	5
7.5	150	4

The actual waypoint controller used for the simulation runs and study will be presented next. The waypoint controller was developed in Simulink as part of a Naval Postgraduate School (NPS) module coursework, ME3720 Introduction to Unmanned Systems. Figure 28 depicts the Simulink model of the waypoint controller. There are four main blocks in the model, which are circled in red. They are namely the Kingfisher USV model, waypoint tracker, cross-track error controller and heading controller. Figure 29 depicts the details of the Kingfisher USV model. The blocks that are circled in red are the ROS topics that are published and subscribed by the Kingfisher USV model. From the subscribed topics, the Kingfisher USV model receives the current USV platform data in Gazebo and after some data manipulation, outputs them to the rest of the controllers for guidance command computation. The outputs are namely 1) heading (in the East North Up [ENU] convention), 2) yaw rates (in ENU convention), 3) coordinates of current position in East and North convention and 4) current speed. The model publishes guidance command to the USV in Gazebo with the inputs from the rest of the controllers.

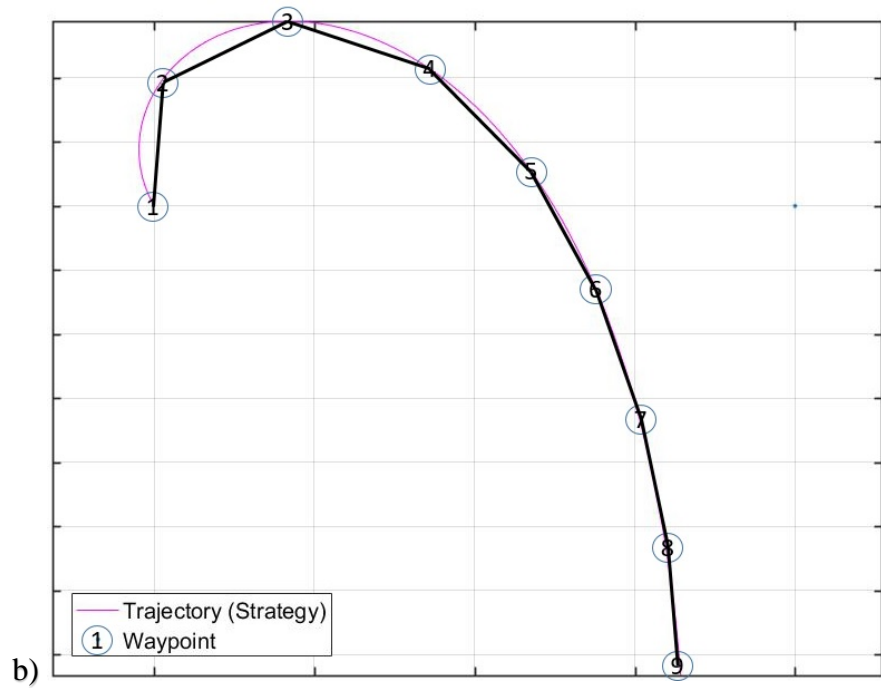
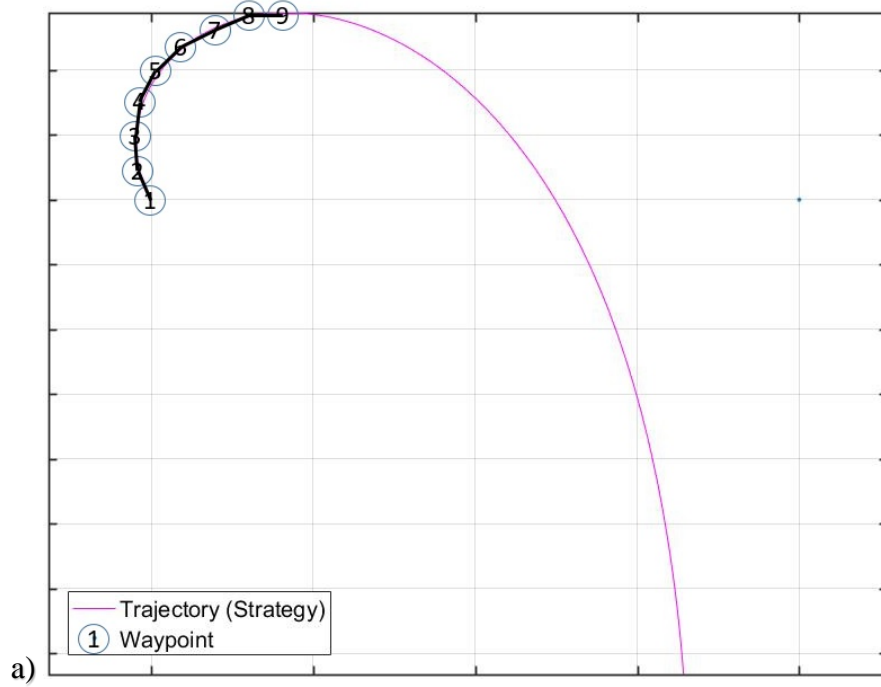


Figure 27. Trajectories of the USV through Various Waypoints, in (a) Short Guidance Command Interval and (b) Long Control Command Interval.



The purpose of the second block, waypoint tracker, ensures that all declared waypoints are circled through. It is important to realize that the USV does not arrive at the waypoints exactly on the spot but within a threshold distance. Once the USV enters the defined threshold radius of the waypoint, the USV is considered to have arrived at the waypoint. The waypoint tracker manages the waypoints according to the following algorithm:

- (1) Initialization step. Read Waypoints File. If (no waypoint found), stop and exit the simulation, else set next waypoint as waypoint 1 (waypoint index = 1) and go to Step 2.
- (2) Recursive step (over waypoints). While (waypoint index < total number of waypoints), check current position. If (current position is within threshold distance of waypoint), increase the waypoint index by 1 else, compute the 1) waypoint speed, 2) along track error, 3) cross-track error, 4) line-of-sight (LoS) heading, and 5) status of simulation and output them for other blocks in the model.

Each waypoint is the position of the USV in the guidance strategy at every  $i^{\text{th}}$  and last control cycle where “ $i$ ” is number of control cycles listed in Table 3. The waypoint speed is kept constant at 1.5m/s for all the simulation runs.

The third block, cross-track error controller, receives LoS heading and cross-track error computed in the waypoint tracker block to compute the desired heading command angle in north east down (NED) convention.

The fourth and last block, heading controller, is used to determine the desired inputs for the thrusters to drive the Kingfisher USV to the desired heading. Figure 30 depicts the details of the heading controller. The output heading from the heading controller is desired to be in north east down (NED) convention. However, the yaw rates and heading received from the Kingfisher USV block is in ENU convention. In order to change the yaw rates and heading to NED convention, the heading angle obtained from the Kingfisher USV block is subtracted by  $90^\circ$  and the yaw rate is corrected with a “-1” gain. The proportional gain of the PID is set to 0.65 and the derivative gain is set to 0.35.

These values were chosen based on a tuning exercise that was conducted on the Kingfisher USV in a water tank. The integral gain was set to 0 since the USV reaches steady state value without any error and hence omitted from the model. However, the integral gain would be necessary if environmental conditions were present.

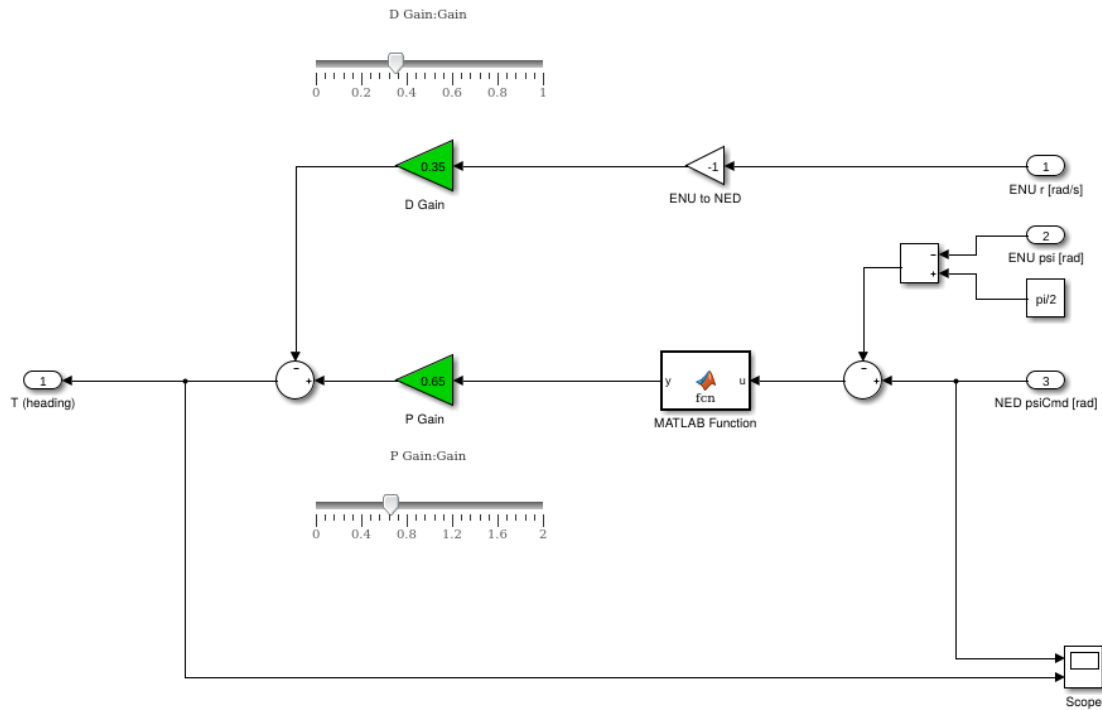


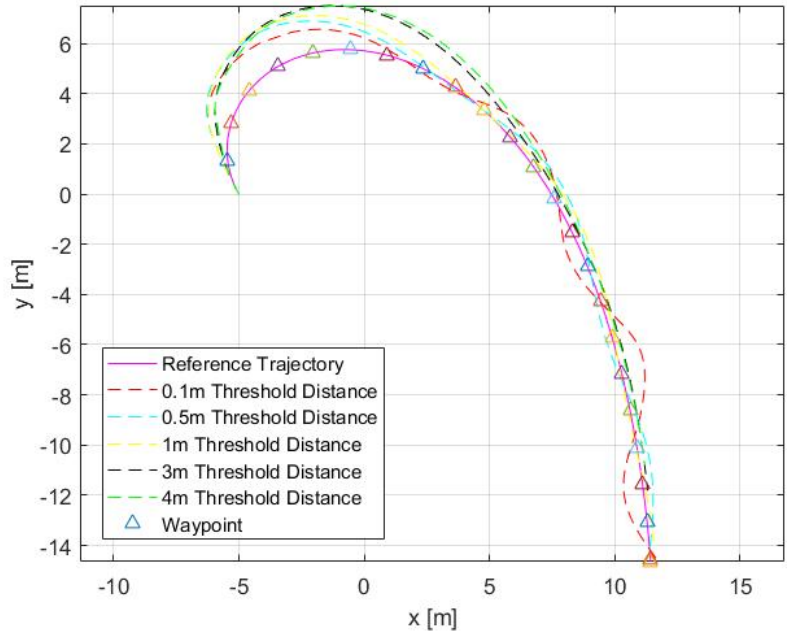
Figure 30. Details of Heading Controller Block.

During the simulation runs, several platform parameters such as speed, heading, and yaw rate were recorded over the simulation time for our study on the effects on different guidance command intervals. The results of the simulation runs and observations from the study of the results will be discussed in the next section.

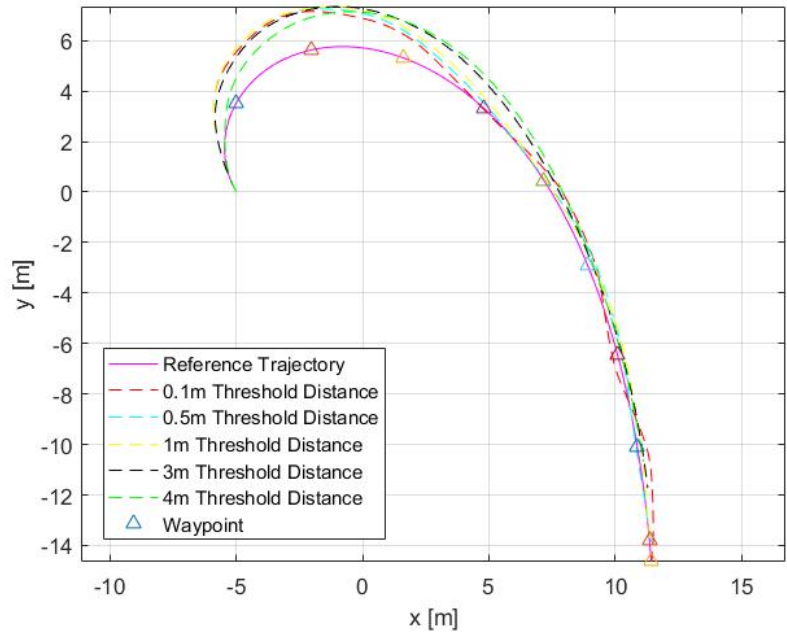
## D. SIMULATION RESULTS

This section presents and discusses the results of several simulations in different guidance command intervals. While the initial goal of the simulation was to study the effects of different guidance command intervals on the trajectories travelled by a USV, the threshold distance of the waypoint is observed to have a significant effect on the trajectories as well. Therefore, together with the study of the effects of different guidance command intervals, the effects of different threshold distances shall be investigated as well. The threshold distances that were selected for this further study were 0.1m, 0.5m, 1m, 3m and 4m. Figure 31 (Cases 1–5) depicts the different threshold distances for each guidance command interval stated in Table 3 for Pursuer 1. The behaviour was observed to be similar for Pursuer 2 and, therefore, the corresponding trajectory graphs for Pursuer 2 were not included in this thesis.

For a more realistic simulation in Gazebo environment, several parameters listed in Section III.C have been modified. The simulations now have the following similar engagement parameters; initial coordinates of Pursuer 1  $\mathbf{R}_{p1} = [-5, 0]^T$  m, initial coordinates of Pursuer 2  $\mathbf{R}_{p2} = [5, 0]^T$  m, initial coordinates of non-maneuvering moving target  $\mathbf{R}_T = [15, 0]^T$  m, final desired angle of Pursuer 1 intercept point with respect to target's heading  $\theta_{p1-T} = \frac{\pi}{4}$ , final desired angle of Pursuer 2 intercept point with respect to target's heading  $\theta_{p2-T} = -\frac{3\pi}{4}$ , final desired range of Pursuer 1 intercept point from target  $R_{p1-T} = 5$  m and final desired range of Pursuer 2 intercept point from target  $R_{p2-T} = 5$  m. The two pursuers in each simulation shall have a different initial heading but same speed. The initial velocity vector of Pursuer 1 shall be  $\mathbf{V}_{p1} = 1.5 * \left[ \cos\left(\frac{2\pi}{3}\right), \sin\left(\frac{2\pi}{3}\right) \right]^T$  m/s and the initial velocity vector of Pursuer 2 shall be  $\mathbf{V}_{p2} = 1.5 * \left[ \cos\left(\frac{3\pi}{4}\right), \sin\left(\frac{3\pi}{4}\right) \right]^T$  m/s.

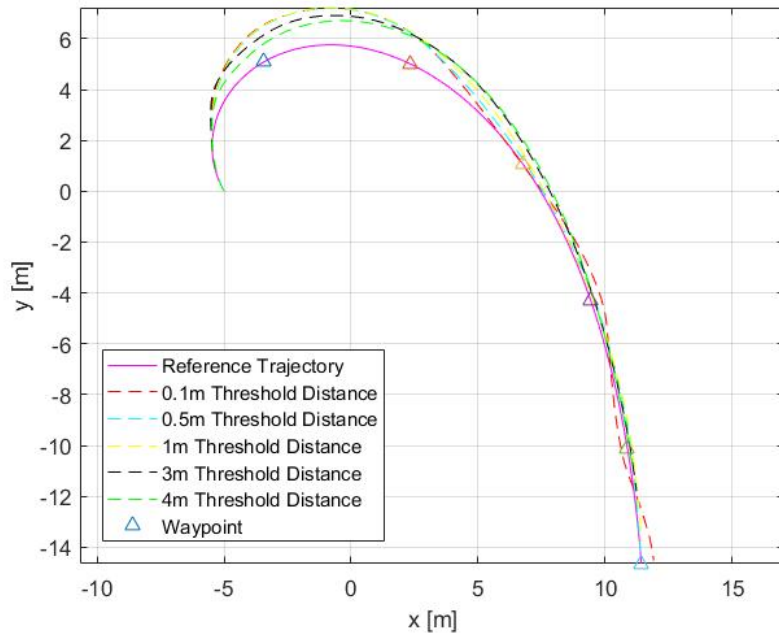


a)

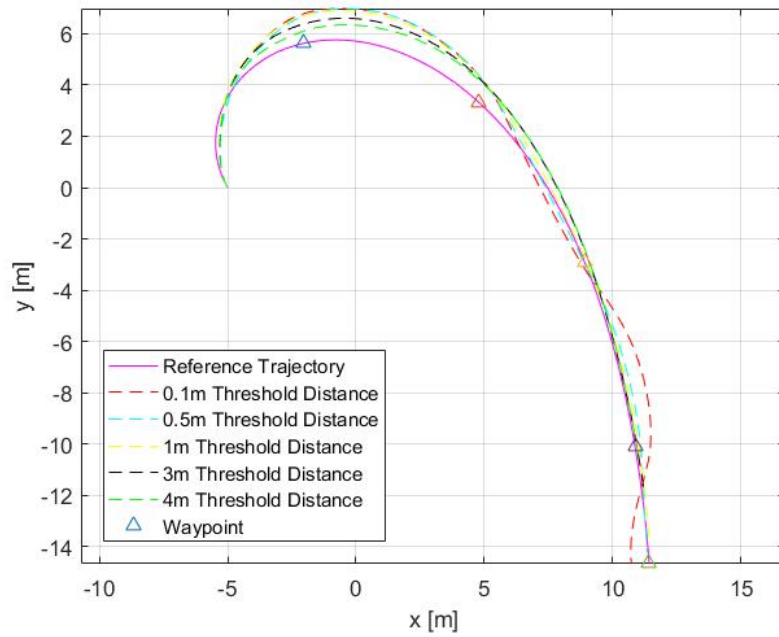


b)

Figure 31. Trajectories of Pursuer 1 with Different Threshold Distances for Different Guidance Command Intervals (Cases 1–5).

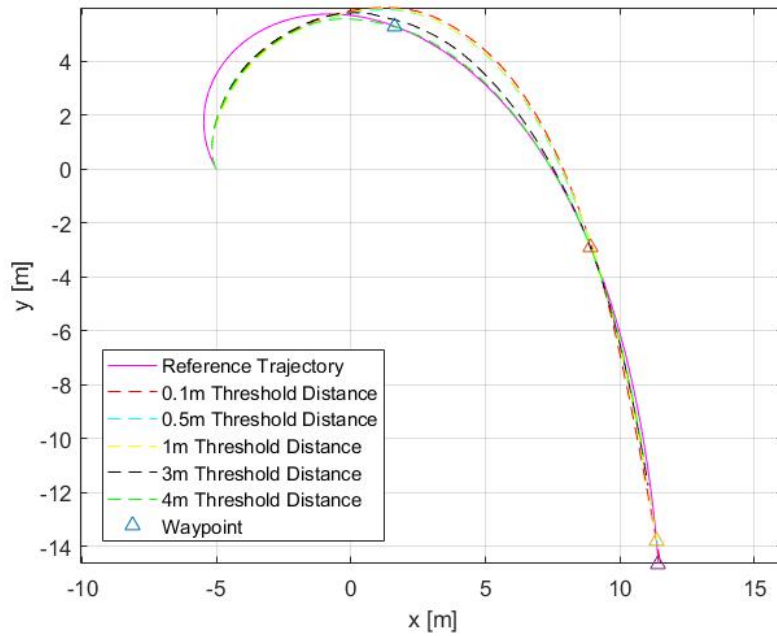


c)



d)

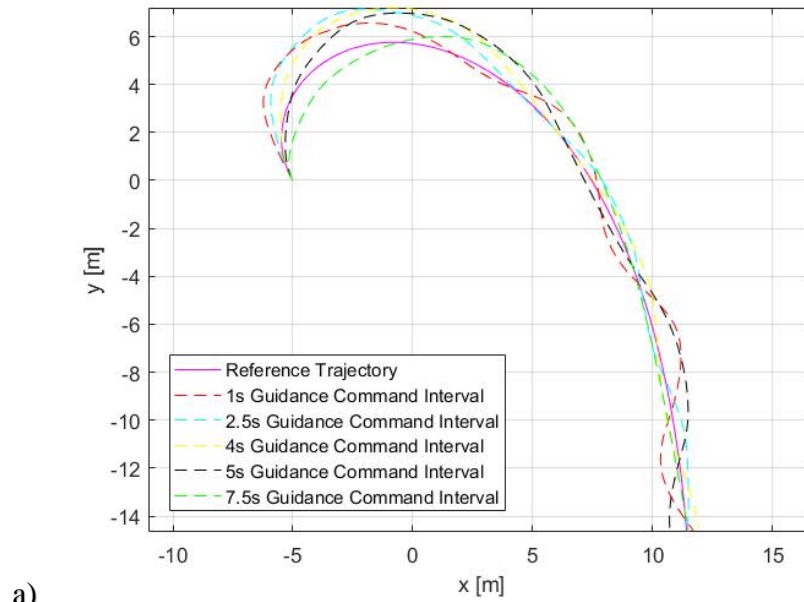
Figure 31 cont'd. Trajectories of Pursuer 1 with Different Threshold Distances for Different Guidance Command Intervals (Cases 1–5).



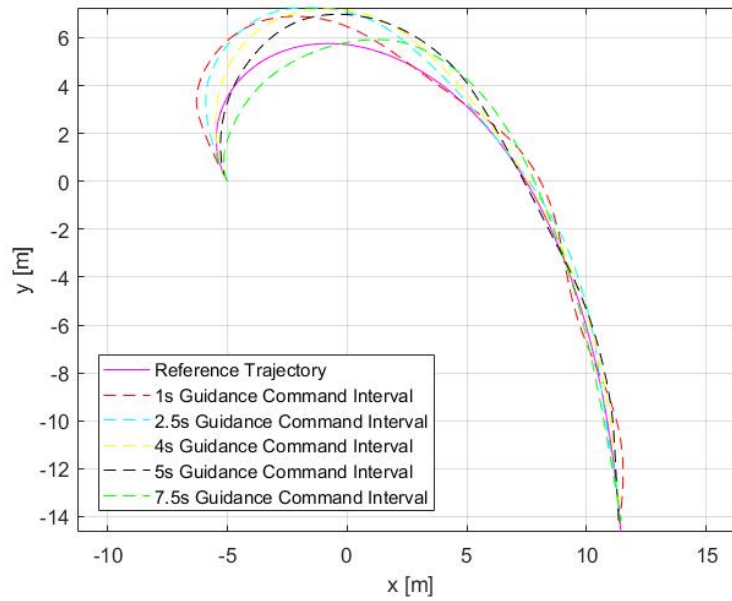
e) Figure 31 cont'd. Trajectories of Pursuer 1 with Different Threshold Distances for Different Guidance Command Intervals (Cases 1–5).

The results demonstrated that it is not necessarily always the right approach to define a stringent threshold distance. One would expect that a small threshold distance of 0.1m would yield the best result against the reference trajectory. However, it is apparent that the trajectory travelled by the USV in the various graphs with a defined threshold distance of 0.1m is not as smooth and direct as other threshold distances tested. This can be attributed to the lack of terminal angle control at each waypoint due to the waypoint controller used for the simulation. The heading controller tends to over correct the USV's heading after its arrival at a waypoint, leading to an undesired approach angle at the next waypoint. This cycle continues until the USV reaches its final waypoint, resulting in the S-shape path at times. This phenomenon is prominent in Case 1, and remains apparent in Cases 2–4. Even a threshold distance of 0.5m for 1s guidance command interval results in a slight S-shape path toward the end of the trajectory, as shown in Case 2. Therefore, defining a stringent threshold distance using a simple waypoint controller without heading control at each waypoint produces a less than desired trajectory/result. However, defining an over-relaxed threshold distance provides another set of problems as well.

Figure 32 (Cases 6–10) demonstrates exactly the problem by overlaying all trajectories with the same threshold distance.

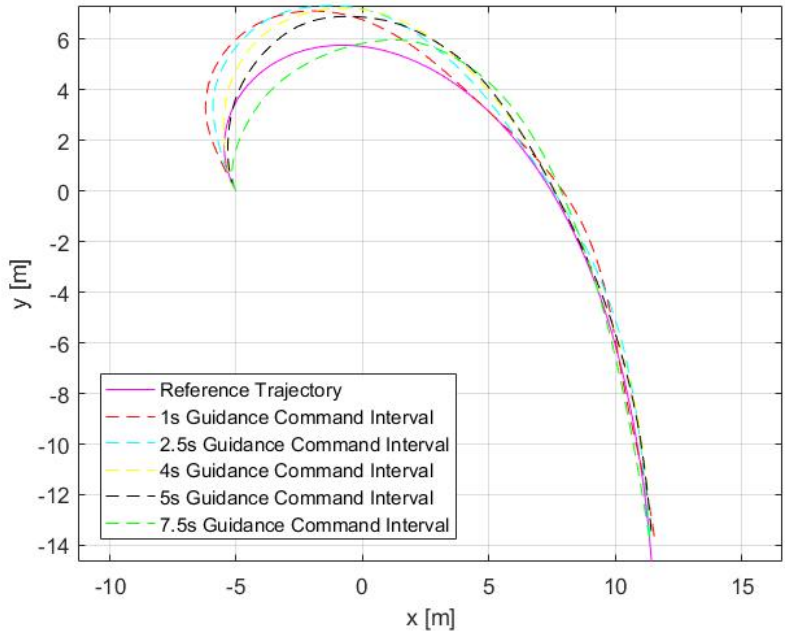


a)

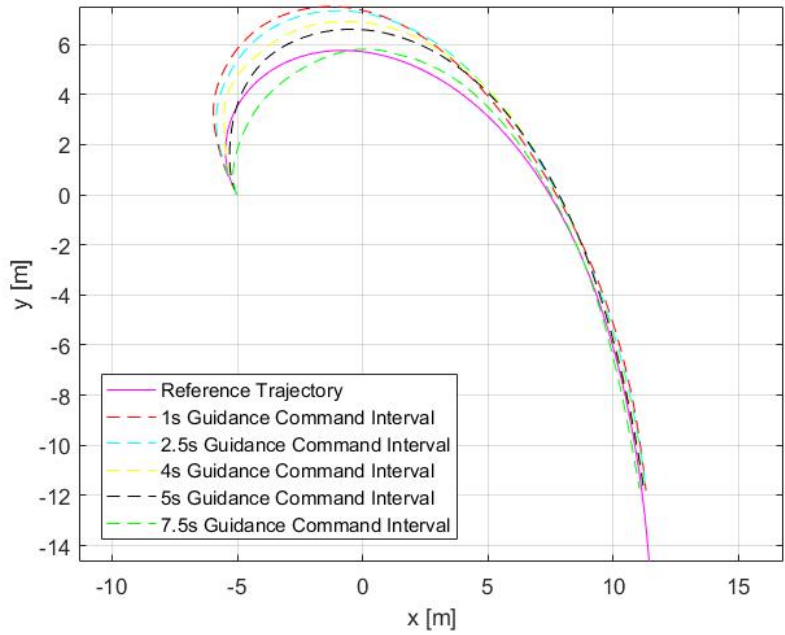


b)

Figure 32. Trajectories of Pursuer 1 with Similar Threshold Distances for Different Guidance Command Intervals (Cases 6–10).

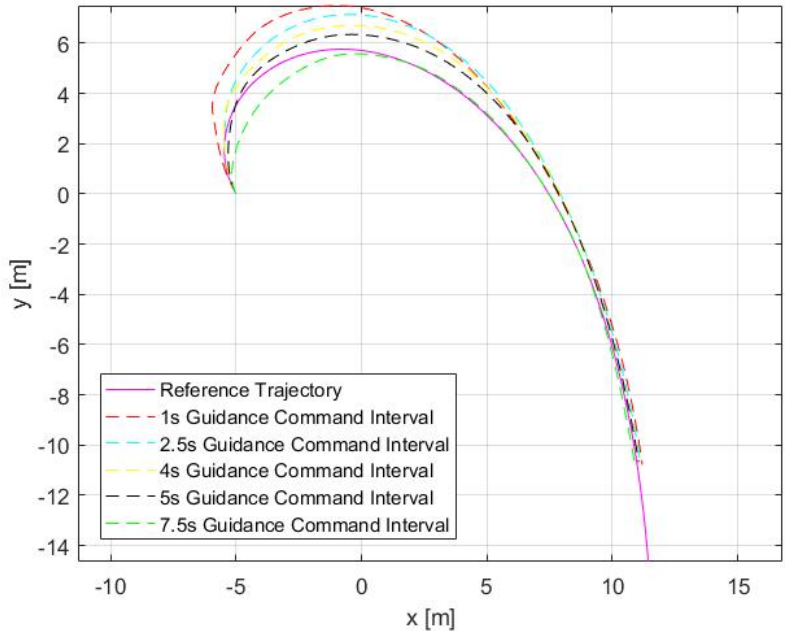


c)



d)

Figure 32 cont'd. Trajectories of Pursuer 1 with Similar Threshold Distances for Different Guidance Command Intervals (Cases 6–10).



e) Figure 32 cont'd. Trajectories of Pursuer 1 with Similar Threshold Distances for Different Guidance Command Intervals (Cases 6–10).

Figure 32 starts with trajectories of the USV of different guidance command intervals with 0.1m threshold distance (Case 6), and ends with trajectories of different guidance command intervals with 4m threshold distance (Case 10). It is noticeable that the trajectories are ending prematurely in increasing order as the threshold distance increases. This phenomenon is understandable as the waypoint controller stops the simulation as soon as the USV falls within the radius of the defined threshold distance. By defining a large threshold distance, the final angle of pursuer intercept point with respect to target's heading and final range of pursuer intercept point from target will be affected. Figure 33 illustrates a simple and approximate case on the difference between the final heading and the final range of a pursuer from target from the final desired heading and range. This simple illustration assumes that Pursuer 2 is travelling to the final waypoint in a straight path from North to South from the previous waypoint.

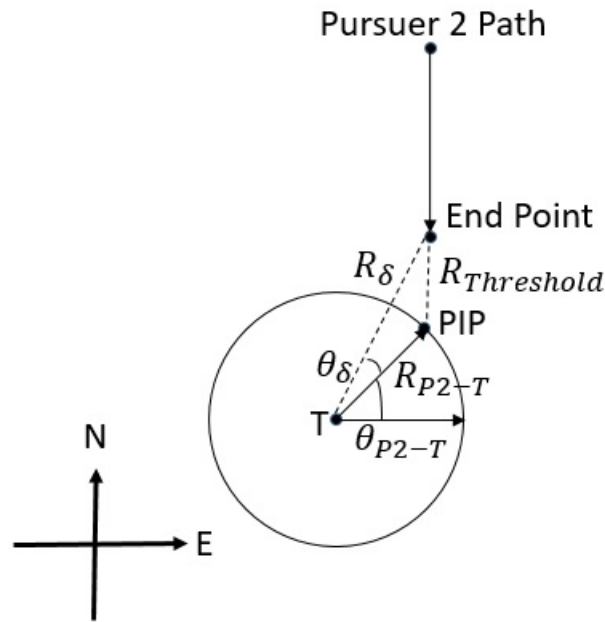


Figure 33. Illustration on the Effects of Threshold Distance on the Final Heading and Range from Target.

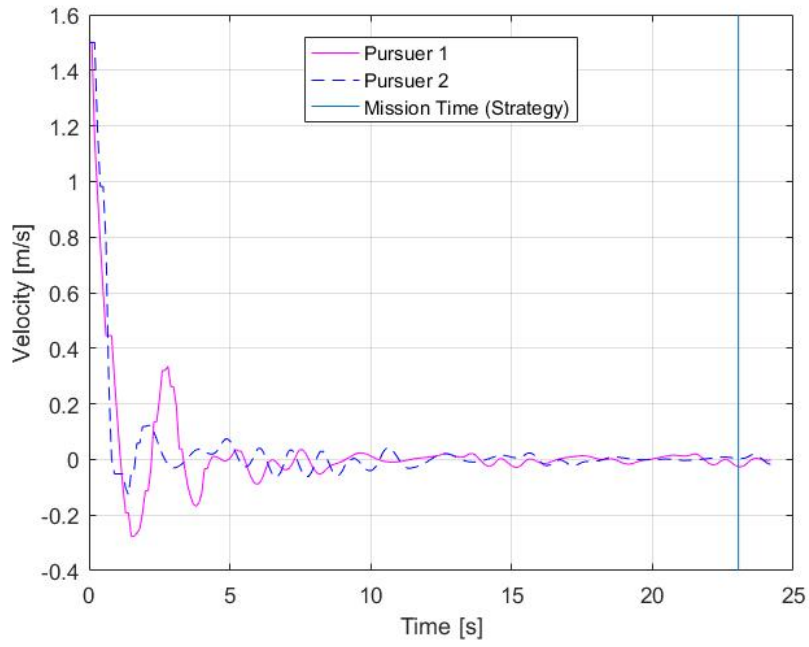
Recall that the final desired angle of Pursuer 2 intercept point with respect to target's heading  $\theta_{P2-T} = -\frac{\pi}{4}$  and final desired range of Pursuer 2 intercept point from target  $R_{P2-T} = 5\text{m}$  have been defined at the start of this section.  $\theta_\delta$  represents the error in final heading as compared to the final desired angle,  $R_\delta$  represents the error in final range from the target as compared to the final desired range and  $R_{Threshold}$  represents the threshold distance defined. Table 4 provides an overview on the percentage of error for final heading and range from the final desired heading and range from target based on the defined threshold distance.

Table 4. Overview on the Percentage or Error for Final Heading and Range with Different Threshold Distances.

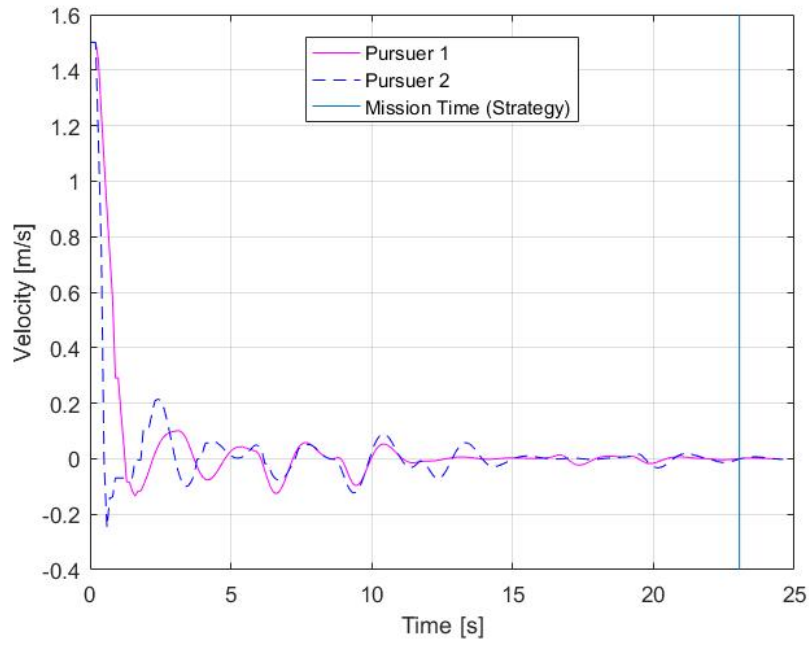
Threshold Distance, $R_{Threshold}$ (m)	Error in Final Range, $R_s$ (m)	Percentage Error in Final Range (%)	Error in Final Heading, $\theta_s$ (°)	Percentage Error in Final Heading (%)
0.1	$\approx 0.071$	1.42	$\approx 0.799$	1.78
0.5	$\approx 0.365$	<b><u>7.3</u></b>	$\approx 3.778$	<b><u>8.40</u></b>
1	$\approx 0.751$	15.02	$\approx 7.063$	15.70
3	$\approx 2.431$	48.62	$\approx 16.588$	36.86
4	$\approx 3.324$	66.48	$\approx 19.865$	44.14

From Table 4, the error in final range can be up to 66% of the final desired range and the error in final heading can be up to 44% of the final desired heading based on the threshold distances tested. A threshold distance of 0.5m yields error of less than 10% for both final range and heading which is acceptable in this thesis. Furthermore, the trajectories travelled with 0.5m threshold distance appear to be largely satisfactory. Hence, the next study on the effects of guidance command intervals on the different trajectories shall be concentrated on the trajectories travelled with a 0.5m threshold distance.

An examination shall be performed on the speed and yaw rate profiles of the USVs to investigate the effects of guidance command intervals. Velocity, heading, and yaw rate profiles of both pursuers for different guidance command intervals, respectively, are depicted in Figures 34–36. The five different cases for Figures 34–36 always start with a case with 1s guidance command interval and ending with a case of 7.5s guidance command interval with 2.5, 4s, and 5s guidance command interval cases in ascending order in between.

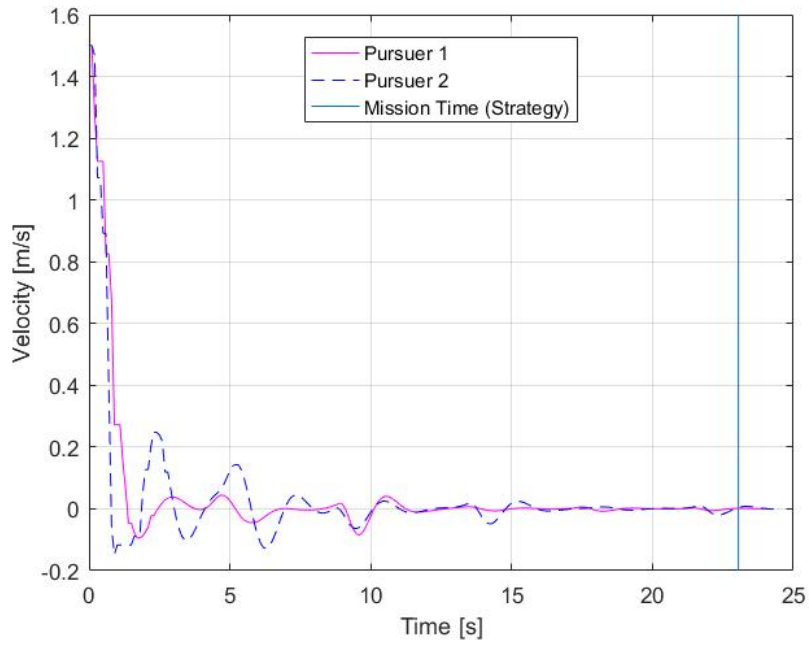


a)

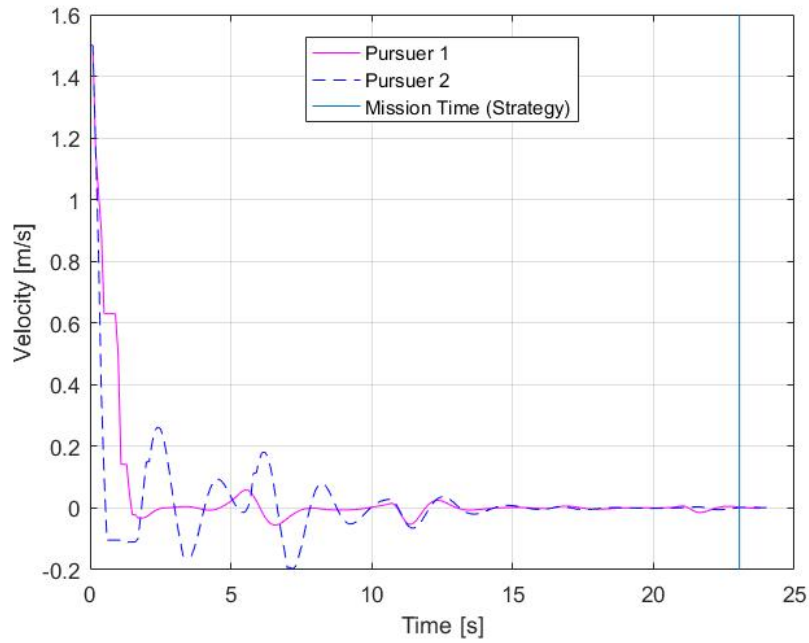


b)

Figure 34. Velocity Profiles of Both Pursuers for Different Guidance Command Intervals.

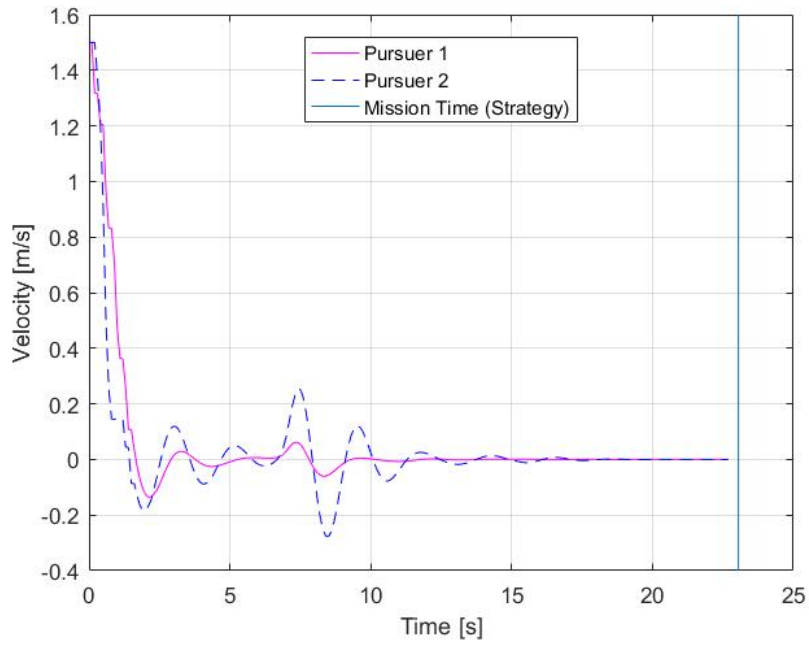


c)

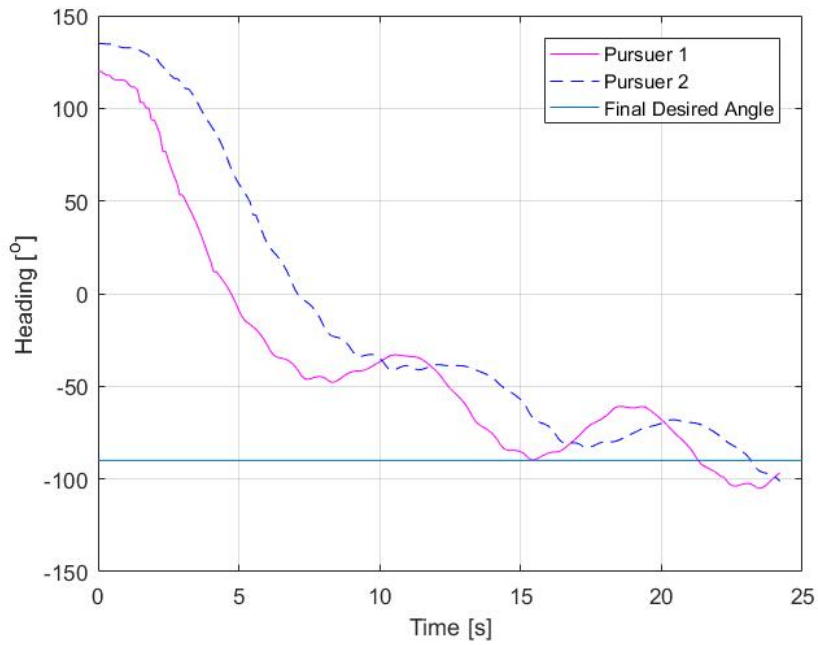


d)

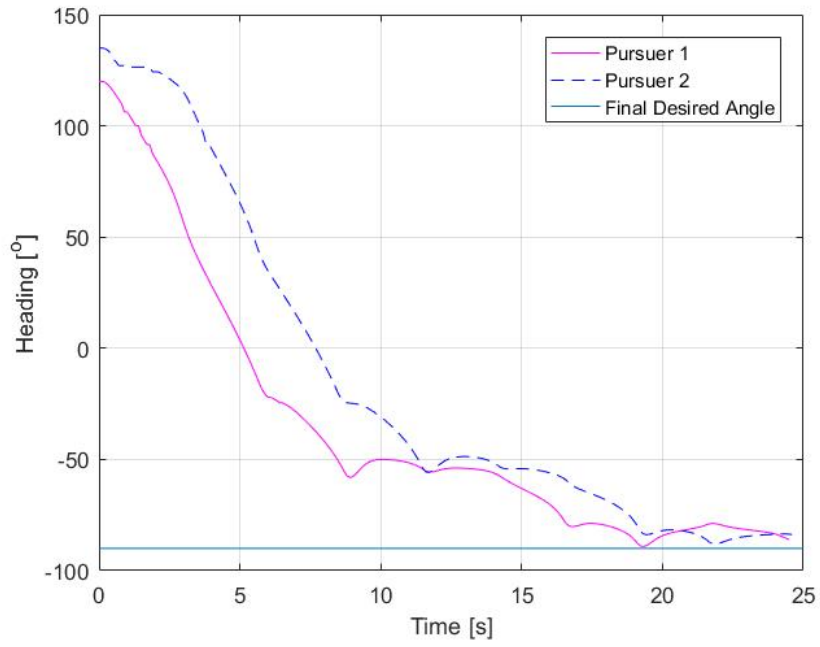
Figure 34 cont'd. Velocity Profiles of Both Pursuers for Different Guidance Command Intervals.



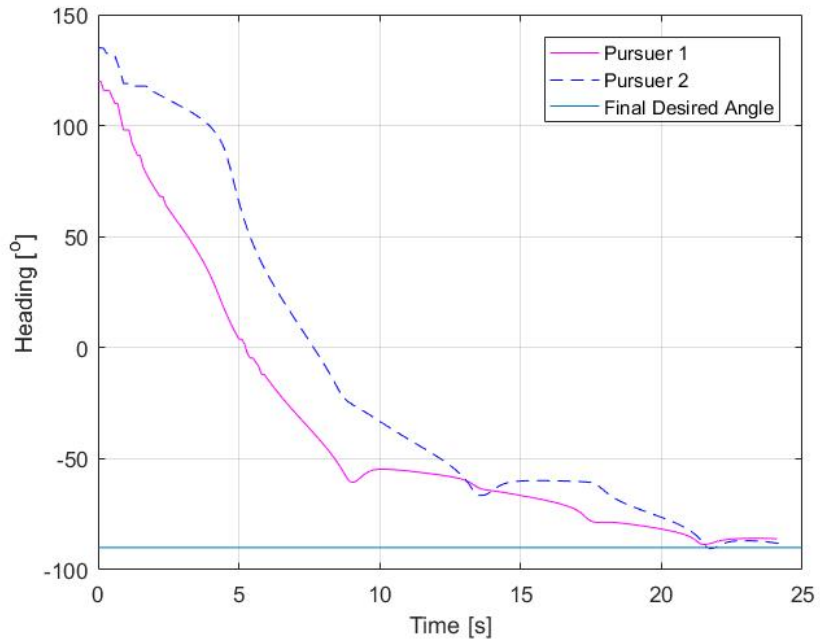
e) Figure 34 cont'd. Velocity Profiles of Both Pursuers for Different Guidance Command Intervals.



a) Figure 35. Heading Profiles of Both Pursuers for Different Guidance Command Intervals.

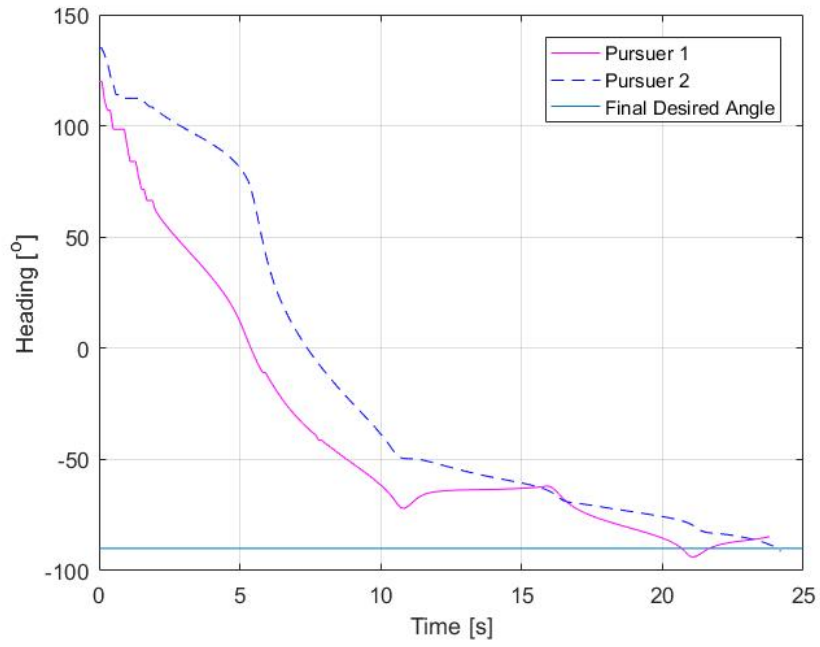


b)

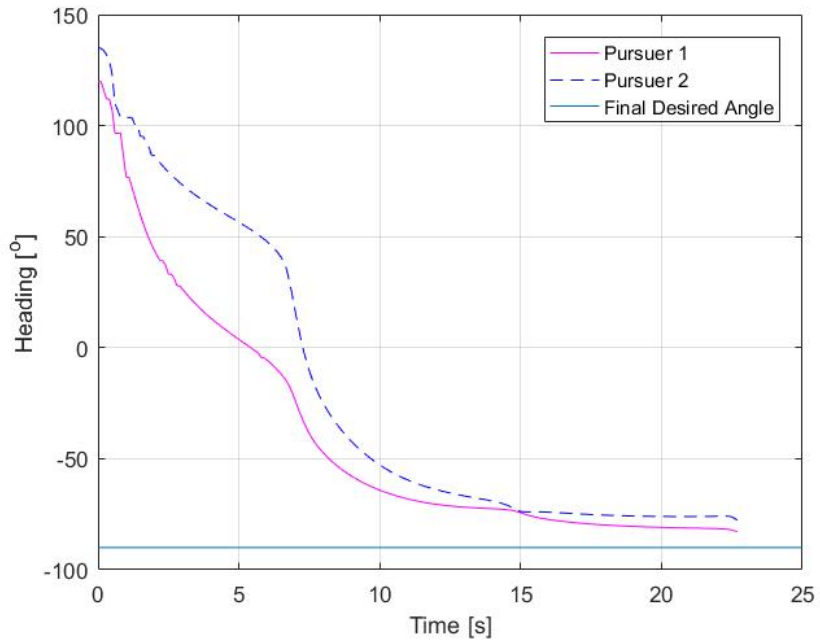


c)

Figure 35 cont'd. Heading Profiles of Both Pursuers for Different Guidance Command Intervals.



d)



e)

Figure 35 cont'd. Heading Profiles of Both Pursuers for Different Guidance Command Intervals.

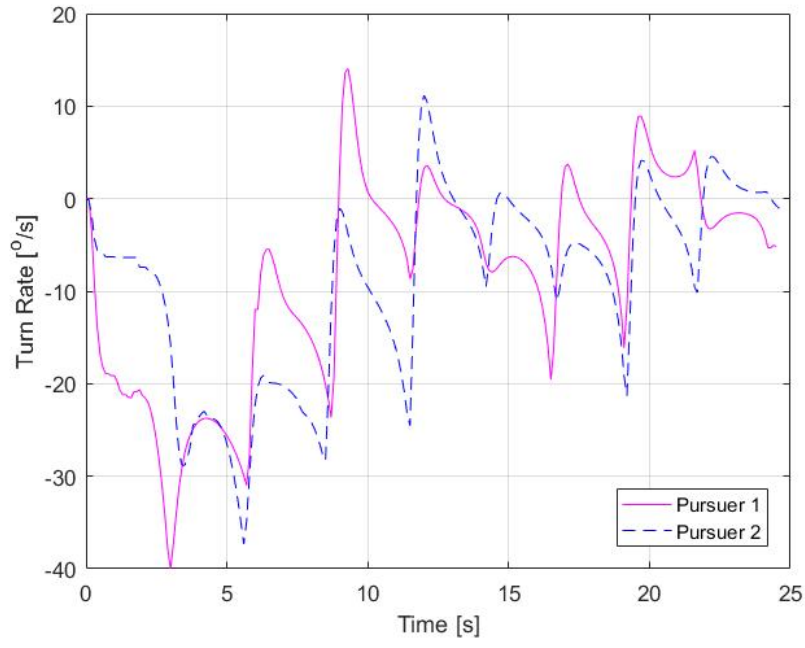
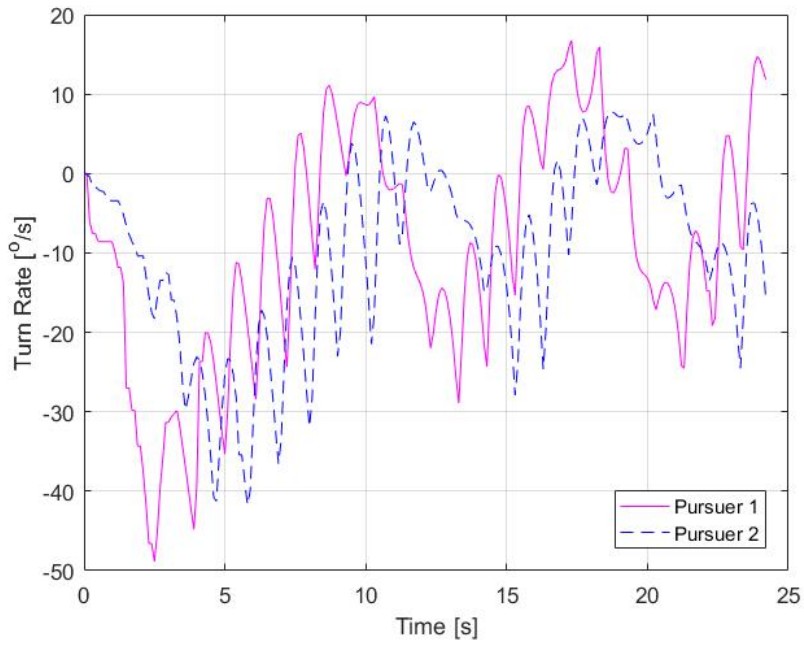
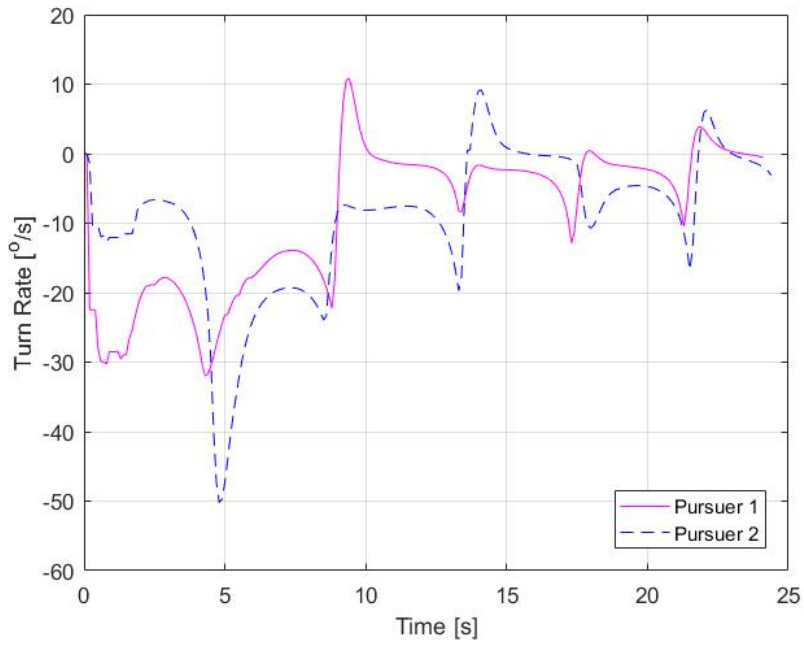
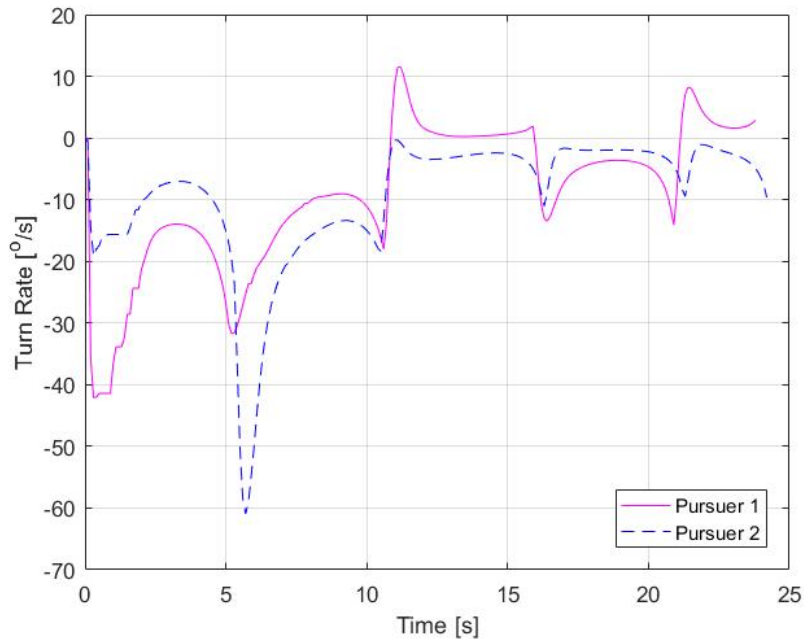


Figure 36. Yaw Rate Profiles of Both Pursuers for Different Guidance Command Intervals.

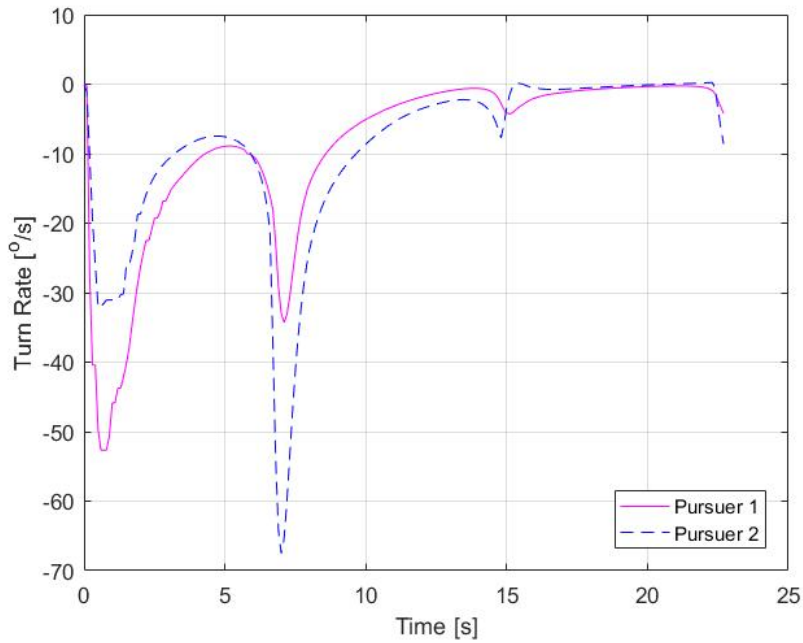


c)



d)

Figure 36 cont'd. Yaw Rate Profiles of Both Pursuers for Different Guidance Command Intervals.



e)

Figure 36 cont'd. Yaw Rate Profiles of Both Pursuers for Different Guidance Command Intervals.

The vertical line in Figure 34 marks the expected pursuers' mission time (23.05s) per total number of control cycles (461 as stated in Section IV.C) during the guidance generation. Recall that each control cycle is 0.05s as stated in Section III.C. It can be observed that the pursuers arrive at the target (observed from the spikes in the velocity curve to determine motion) in decreasing mission time as the guidance command interval increases. This is due to the pursuers travelling shorter trajectories, apparent in all Figure 32 cases. Since the objective of the guidance command is to control a pursuer to travel a trajectory as similar as possible to the reference trajectory, it is highly undesirable to have a shorter than acceptable actual mission time.

Next, the horizontal line in Figure 39 marks the final desired heading, which is parallel to the target's trajectory at  $-90^\circ$ . The pursuers in all Figure 35 cases are observed to converge approximately to the final desired heading. This is due to the gentle curve gradient towards the end of the reference trajectory, allowing the pursuers to travel to the final waypoint from the previous waypoint in a relatively straight path. However, one should expect the results of pursuers' final heading to be worse for a case of steep curve

gradient towards the end of the reference trajectory with shorter guidance command interval as compared to a longer guidance command interval. This is due to the over correction of heading by the heading controller as mentioned earlier in this section.

The maximum yaw rate shown in Figure 36 increases as the guidance command interval increases. This is expected since the waypoints are further apart with a larger guidance command interval, which some require sharp turns to achieve the approach angle to the next waypoint and hence, the higher yaw rate observed. The design and characteristics of USVs are out of the scope of this thesis. However, it is important to keep in mind that USVs' platform characteristics such as yaw rate should be considered when selecting guidance command interval.

## **E. DISCUSSION OF SIMULATION RESULTS**

The study of the effects of different guidance command intervals led to another study on the effects of different threshold distance. Depending on the controller, a stringent threshold distance might not necessary yields the best result. However, over relaxing the defined threshold distances produce results with high percentage of error from the PIP. Different guidance command intervals pose a different set of problems as well. Large guidance command intervals result in the pursuers taking a shorter path to the PIP and arriving at the PIP much earlier than the expected mission time. Large guidance command intervals also possibly require the platform to be capable of turning sharply or high yaw rate. Again, depending on the controller, a short command interval might result in over correction of the robot's heading when travelling to the next waypoint, resulting in a trajectory that is not as smooth as the reference trajectory. There is no definite conclusion or recommendations to the "best" guidance command interval or threshold distance for the USVs, or any other unmanned system and robots. The expected trajectory of the unmanned platform, the platform characteristics and the type of controller used for the system, shall be the main consideration points when determining the optimal guidance command interval or threshold distance.

THIS PAGE INTENTIONALLY LEFT BLANK

## V. CONCLUSION AND FUTURE WORK

Maritime interdiction operations have always been a great challenge for the Coast Guard. The need to carry out interdiction operations safely with high success rate, coupled with the limited manpower and assets, proves to be a daunting task. Fortunately, the advancement in unmanned technology is an answer to the problem. The autonomous USVs are better suited for the “dull, dirty, or dangerous missions” rather than manned systems (Unmanned Aerial Vehicle Systems Association 2008). Unmanned platforms have proven in recent years to be capable and reliable and preferred to manned platforms in providing additional “advantages and contributions beyond replacing humans in dull, dirty and dangerous roles” (Hernandez 2016b).

In this thesis, we apply systems engineering approach to design a solution (i.e., swarming USVs system) for the operation need. The DOD SEP model of 2014 was employed to provide the framework for the development of the solution and scope of the thesis up to the DT&E process. Through the functional and requirement analysis process, percentage of computation time for guidance generation against the actual mission time and percentage of positional and heading error from the predicted intercept point were identified as the key design parameters for the guidance strategy and control.

A coordinated trajectory-shaping guidance strategy for multiple pursuers tasked to execute a synchronous interdiction of a non-maneuvering moving target in an angle-constrained approach was developed. PN-based methods were selected based on its simple but elegant and efficient user-friendly structure of a guidance command. Simulation results show that the guidance generation requires less than 3% of the actual mission time with interpretative execution instructions (not compiled code). This implies that the algorithm can be run in real-time implementation with compiled code that runs about 100 times faster (Yakimenko 2000). A study was conducted together with the development of the coordinated trajectory-shaping guidance strategy to investigate the effects of different guidance command intervals and threshold distances on the trajectories travelled by the USVs when the algorithm is implemented on an onboard autopilot. The study was conducted in Gazebo, a high-fidelity simulation environment.

The effects due to different guidance command intervals and threshold distances were clear. The shortest guidance command interval and threshold distance may not necessary produce the least positional and heading errors from the predicted intercept point for every unmanned application. The optimal guidance command interval or threshold distance for an unmanned system depends on the expected trajectory of the unmanned platform, the platform characteristics and the type of controller used for the system. Overall, this thesis proves that using USVs with the appropriate intercept guidance for the maritime interdiction missions is a viable alternative/complement to the current operations involving only manned vessels.

Future research involves including an inter-pursuer collision avoidance capability, collision avoidance with surrounding objects/obstacles, and transitioning to maritime testing the developed algorithms using the fleet of USVs available at the NPS.

## LIST OF REFERENCES

- AcqNotes. 2016. “Measures of Effectiveness (MOE).”  
<http://www.acqnotes.com/acqnote/careerfields/te-measures-of-effectiveness>.
- Bardhan, Rajarshi, and Debasish Ghose. 2015. “Nonlinear Differential Games-Based Impact-Angle-Constrained Guidance.” *Journal of Guidance, Control, and Dynamics* 38(3): 384–402.
- Cho, Hangju, Chang-Kyung Ryoo, Antonios Tsourdos, and Brian White. 2014. “Optimal Impact Angle Control Guidance Law Based on Linearization About Collision Triangle.” *Journal of Guidance, Control, and Dynamics* 37(3): 958–964.
- Defense Acquisition University. 2017. “Systems Engineering Process.”  
<https://dap.dau.mil/acquipedia/Pages/ArticleDetails.aspx?aid=9c591ad6-8f69-49dd-a61d-4096e7b3086c>.
- Dhananjay, Narayanachar, and Debasish Ghose. 2014. “Accurate time-to-go estimation for proportional navigation guidance.” *Journal of Guidance, Control, and Dynamics* 37(4): 1378–1383.
- Drone Trend. 2014. “Caracas – Les futurs drones de la Navy Americaine.”  
<http://www.drone-trend.fr/caracas-drones-navy-americaine-1405>.
- Ghosh, Satadal, Debasish Ghose, and Soumyendu Raha. 2013. “Three Dimensional Retro-PN Based Impact Time Control for Higher Speed Nonmaneuvering Targets.” *Proceedings of IEEE Conference on Decision and Control* IEEE Publ., Piscataway, NJ: 4865–4870.
- . 2016a. “Composite Guidance for Impact Angle Control Against Higher Speed Targets.” *Journal of Guidance, Control, and Dynamics* 39(1): 98–117.
- . 2016b. “Unified Time-to-go Algorithms for Proportional Navigation Class of Guidance.” *Journal of Guidance, Control, and Dynamics* 39(6): 1188–1205.
- Ghosh, Satadal, Oleg A. Yakimenko, D. T. Davis, and T. H. Chung. 2017. “Unmanned Aerial Vehicle Guidance for an All-Aspect Approach to a Stationary Point.” Accepted in *AIAA Journal of Guidance, Control, and Dynamics*.
- Gazebo. 2016. “Beginner: Overview.”  
[http://gazebosim.org/tutorials?cat=guided\\_b&tut=guided\\_b1](http://gazebosim.org/tutorials?cat=guided_b&tut=guided_b1).
- Generation Robots. 2016. “ROS – Robot Operating System.”  
<http://www.generationrobots.com/blog/en/2016/03/ros-robot-operating-system-2/>.

- Harrison, Gregg A. 2012. “Hybrid Guidance Law for Approach Angle and Time-of-Arrival Control.” *Journal of Guidance, Control, and Dynamics* 35(4): 1104–1114.
- Hernandez, Alejandro 2016a. Fundamentals of Systems Engineering [Lecture notes]. Department of Systems Engineering, Naval Postgraduate School, Monterey, CA.
- . 2016b. Fundamentals of Systems Engineering [Project 4 Instructions]. Department of Systems Engineering, Naval Postgraduate School, Monterey, CA.
- Jeon, In-Soo, Jin-Ik Lee, and Min-Jea Tahk. 2006. “Impact-Time-Control Guidance Law for Anti-Ship Missiles.” *IEEE transactions on Control Systems Technology* 14(2): 260–266.
- . 2010. “Homing Guidance Law for Cooperative Attack of Multiple Missiles.” *Journal of Guidance, Control, and Dynamics* 33(1): 275–280.
- Kim, Byung Soo, Gyu-In Jee, and Hyung Seok Han. 1998. “Biased PNG Law for Impact with Angular Constraint.” *IEEE transactions on Aerospace and Electronic Systems* 34(1): 277–288.
- Kim, M., and Kelly V. Grider. 1973. “Terminal Guidance for Impact Attitude Angle Constrained Flight Trajectories.” *IEEE transactions on Aerospace and Electronic Systems* 9(6): 852–859.
- Kumar, Shashi Ranjan, and Debasish Ghose. 2015. “Impact Time and Angle Control Guidance.” *AIAA Guidance, Navigation, and Control Conference, AIAA SciTech Forum AIAA 2015–0616*.
- Kumar, Shashi Ranjan, Sachit Rao, and Debasish Ghose. 2014. “Nonsingular Terminal Sliding Mode Guidance with Impact Angle Constraints.” *Journal of Guidance, Control, and Dynamics* 37(4): 1114–1130.
- Lee, Chang-Hun, Tae-Hun Kim, and Min-Jea Tahk. 2013. “Interception Angle Control Guidance Using Proportional Navigation with Error Feedback.” *Journal of Guidance, Control, and Dynamics* 36(5): 1556–1561.
- Lee, Jin-Ik, In-Soo Jeon, and Min-Jea Tahk. 2006. “Guidance Law to Control Impact Time and Angle.” *IEEE Aerospace and Electronic Systems Magazine* 43(1): 301–310.
- Leonard, Simon, Azad Shademan, Yonjae Kim, Axel Krieger, and Peter C. W. Kim. 2014. “Smart Tissue Anastomosis Robot (STAR): Accuracy Evaluation for Supervisory Suturing Using Near-infrared Fluorescent Markers.” *IEEE International Conference on Robotics and Automation (ICRA)*.

- MathWorks. 2015. “Exchange Data with ROS Publishers and Subscribers.” <https://www.mathworks.com/help/robotics/examples/exchange-data-with-ros-publishers-and-subscribers.html>.
- NASA Jet Propulsion Laboratory. 2014. “Autonomy and Situational Awareness for UMS.” <https://www-robotics.jpl.nasa.gov/tasks/showBrowseImage.cfm?TaskID=271&tdaID=700075>.
- Naval Drones. 2016. “CARACaS (Control Architecture for Robotic Agent Command and Sensing).” <http://www.navaldrones.com/CARACAS.html>.
- NPS Wiki. 2017. “Gazebo Simulation of Kingfisher/Heron USV.” <https://wiki.nps.edu/pages/viewpage.action?pageId=818282511>.
- Office of the Under Secretary of Defense for Acquisition, Technology and Logistics. 2011. “Unmanned Systems Integrated Roadmap: FY 2011–2036.” <http://www.acq.osd.mil/sts/docs/Unmanned%20Systems%20Integrated%20Roadmap%20FY2011-2036.pdf>.
- Ohlmeyer, Ernest J. 2003. “Control of Terminal Engagement Geometry Using Generalized Vector Explicit Guidance.” *Proc. American Control Conference*, IEEE Publ., Piscataway, NJ: 396–401.
- Rao, Sachit, and Debasish Ghose. 2013. “Terminal Impact Angle Constrained Guidance Laws Using Variable Structure Systems Theory.” *IEEE transactions on Control Systems Technology* 21(6): 2350–2359.
- Ratnoo, Ashwini, and Debasish Ghose. 2008. “Impact Angle Constrained Interception of Stationary Targets.” *Journal of Guidance, Control, and Dynamics* 31(6): 1817–1822.
- . 2010. “Impact Angle Constrained Guidance Against Nonstationary Nonmaneuvering Targets.” *Journal of Guidance, Control, and Dynamics* 33(1): 1556–1561.
- Raytheon. 2008. “Phalanx Close-In Weapon System.” <http://www.raytheon.com/capabilities/products/phalanx/>.
- ROS. 2013a. “Core Components.” <http://www.ros.org/core-components/>.
- . 2013b. “About ROS.” <http://www.ros.org/about-ros/>.
- ROS Wiki. 2014. “Introduction.” <http://wiki.ros.org/ROS/Introduction>.
- Ryoo, Chang-Kyung, Hangju Cho, and Min-Jea Tahk. 2006. “Time-to-Go Weighted Optimal Guidance with Impact Angle Constraints.” *IEEE transactions on Aerospace and Electronic Systems* 14(3): 483–492.

- See, Hongze Alex, Satadal Ghosh, and Oleg Yakimenko. 2017. "Towards the Development of an Autonomous Interdiction Capability for Unmanned Aerial Systems." *Proceedings of the 2017 International Conference on Unmanned Aircraft Systems (ICUAS)*: 1378 – 1384.
- Shaferman, Vitaly, and Tal Shima. 2008. "Linear Quadratic Guidance Laws for Imposing a Terminal Intercept Angle." *Journal of Guidance, Control, and Dynamics* 31(5): 1400–1412.
- Shima, Tal. 2011. "Intercept-Angle Guidance." *Journal of Guidance, Control, and Dynamics* 34(2): 484–492.
- Shneydor, Neryahu A. 1998. *Missile Guidance and Pursuit – Kinematics, Dynamics and Control*, 1<sup>st</sup> ed. Sawston, Cambridge: Woodhead Publishing.
- Smalley, David. 2014. "The Future is Now: Navy's Autonomous Swarmboats Can Overwhelm Adversaries." Office of Naval Research.  
<https://www.onr.navy.mil/Media-Center/Press-Releases/2014/autonomous-swarm-boat-unmanned-caracas.aspx>.
- Unmanned Aerial Vehicle Systems Association. 2008. "UAS Application."  
<https://www.uavs.org/applications>.
- Unmanned Systems Technology. 2014. "Kingfisher USV Wins Robobusiness 2014 Game Changer Award."  
<http://www.unmannedsystemstechnology.com/2014/10/kingfisher-usv-wins-robobusiness-2014-game-changer-award/>.
- U.S. Coast Guard. 2012. "Operations" Coast Guard Publication 3–0.  
[https://www.uscg.mil/doctrine/CGPub/CG\\_Pub\\_3\\_0.pdf](https://www.uscg.mil/doctrine/CGPub/CG_Pub_3_0.pdf).
- U.S. Customs and Border Protection. 2017. "CBP, Coast Guard and Puerto Rico Police intercept 4 vessels with 126 undocumented migrants."  
<https://www.cbp.gov/newsroom/local-media-release/cbp-coast-guard-and-puerto-rico-police-intercept-4-vessels-126>.
- U.S. Department of Defense. 2017. "About the Department of Defense (DOD)."  
<https://www.defense.gov/About/>.
- Waymo. 2017. "Technology." Last modified April 25. <https://waymo.com/tech/>.
- Yakimenko, Oleg. 2000. "Direct Method for Rapid Prototyping of Near-Optimal Aircraft Trajectories." *Journal of Guidance, Control, and Dynamics* 23(5): 865–875.
- Yoon, Myung-Gon. 2008. "Relative Circular Navigation Guidance for the Impact Angle Control Problem." *IEEE transactions on Aerospace and Electronic Systems* 44(4): 1449–1463.

## **INITIAL DISTRIBUTION LIST**

1. Defense Technical Information Center  
Ft. Belvoir, Virginia
2. Dudley Knox Library  
Naval Postgraduate School  
Monterey, California